EFSUMB Course Book, 2nd Edition

Editor: Christoph F. Dietrich

Ultrasound of the kidneys and ureter

J. Tuma[1], F. Trinkler[2], F. Záťura[3], B. Nováková[4], A. Serra[1]

[1]Ultrasound Learning Center, Hirslanden Clinic.

[2]Urozentrum Zürich.

[3]Urologic Clinic FN Olomouc.

[4]Clinic of Gastroenterology Košice.

Corresponding author:

Associate Prof. Jan Tuma,

Co-Director EFSUMB Ultrasound Learning Center, Hirslanden Clinic

Witellikerstrasse 40, 8032 Zürich, Switzerland.

Tel. +41 044 387 20 66 Email: Jan.Tuma@hirslanden.ch

Acknowledgment:

The authors thank Tomas Brader for all Illustrations in this chapter and Anthony Rudd for copy editing.

Kidney

Topography

The urogenital system is located retroperitoneally. The kidneys are situated next to liver and spleen, close to psoas muscle and the large abdominal vessels. Dorsal to the kidney lies the iliopsoas muscle, ventrally is either the liver or spleen, medially and ventrally are the large abdominal vessels. The longitudinal axis points from cranial-medial to caudal-lateral and from cranial-dorsal to caudal-ventral. This is important for the accurate measurement of renal length. In its short axis, the renal hilum points in a ventral medial direction [Figure 1–4].

Figure 1 Normal position of kidneys and ureters.

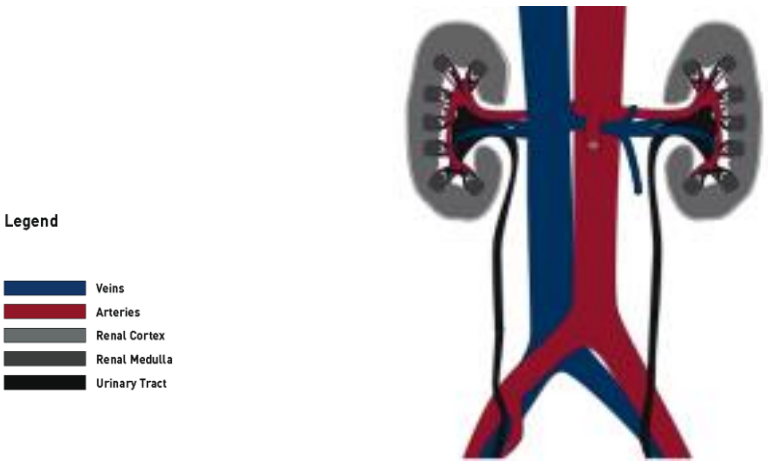

Figure 2 **In the sagittal plane, the longitudinal axis points in a dorsal cranial to ventral caudal direction.**

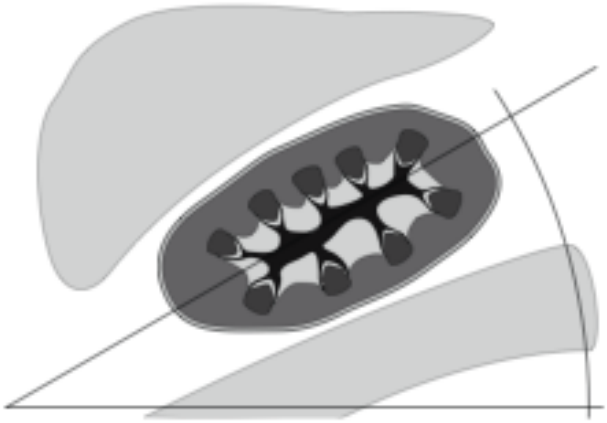

Figure 3 **In the frontal plane, the longitudinal axis points in a medial cranial to lateral caudal direction.**

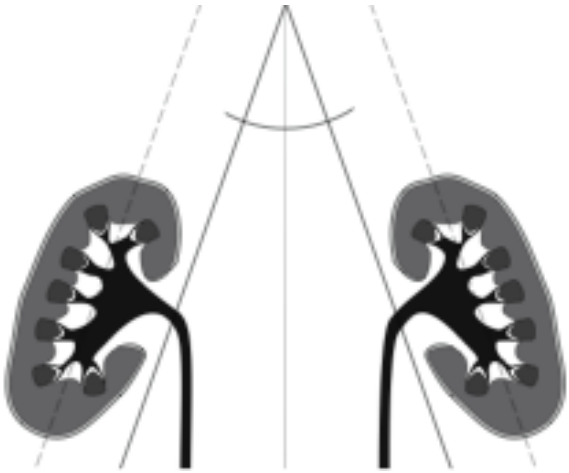

Figure 4 The short axis points in a dorsal lateral to ventral medial direction.

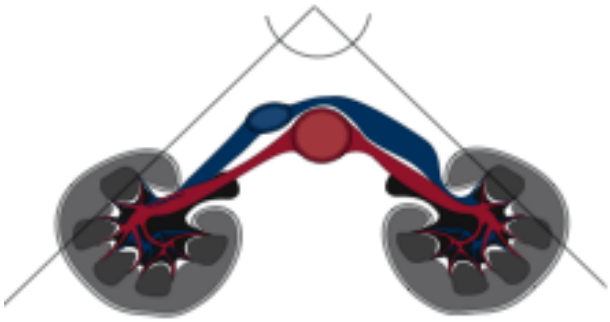

Anatomy

The macroscopic structure of the kidney is well depicted on sonography. In obese patients, the outer kidney capsule limits the perirenal fat body and the inner kidney echogenic capsule represents a kidney contour. The parenchyma can be differentiated in the echogenic renal cortex as well as the 12–15 echo poor pyramids that point conically towards the limit of the kidney sinus. Between the pyramids, the kidney cortex reaches up to the sinus. The bases of the pyramids are limited by the light reflex of the arcuate artery. In the longitudinal axis, the more echogenic and inhomogenous oval kidney sinus can be seen in the middle of the parenchyma; in cross-section it appears semi-circular [Figure 5 and 6].

The renal artery and vein are observed emerging at a right angle from the renal hilum. The right kidney vein merges directly into the vena cava, whereas the left vein first crosses the aorta ventrally. The right renal artery points behind the vena cava to the renal hilum [Figure 1 and 7].

The ureters emerge from the renal hilum caudally. They then proceed along the psoas muscle and cross the iliac vessels to reach the ureteral orifices of the bladder retroperitoneally [Figure 1]. This anatomical course is important when looking for ureteric stones.

The urinary collecting system is easily recognised when there is urinary obstruction. With the patient lying in the prone position, the renal pelvis should be easily visible in most cases. The exit of the ureter can be seen in this position [Figure 8].

The basic functional unit of the kidney is the renal lobule [Figure 9 and 10], which consists of a renal pyramid with the surrounding kidney cortex and is a similar size to a rats kidney, which has one lobule only. In the human kidney between 12 and 15 lobules merge together. Occasionally evidence of this merging (or lobulation) can be seen [Figure 11], especially during childhood, and this is a normal variation [Figure 12].

Figure 5 **Longitudinal view:** right kidney lies behind the liver and lies on m.psoas.

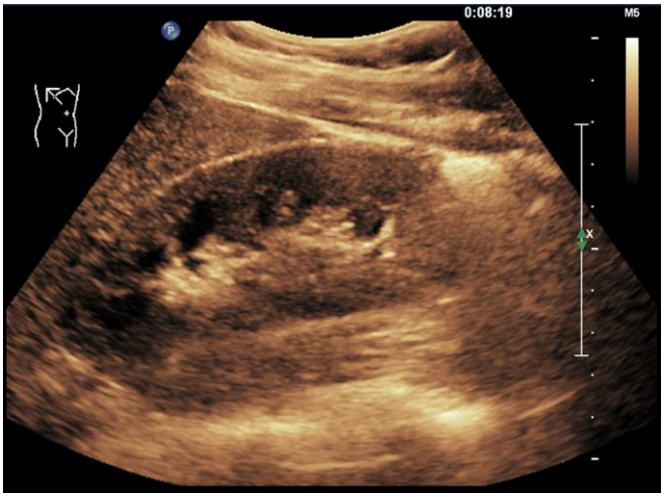

Figure 6 **Cross-section view:** left kidney behind spleen.

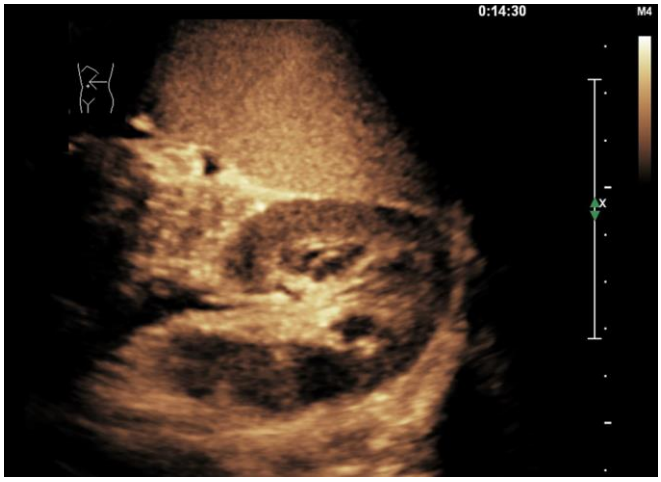

Figure 7 Renal vessels. RRA, right renal artery; LRA, left renal artery.

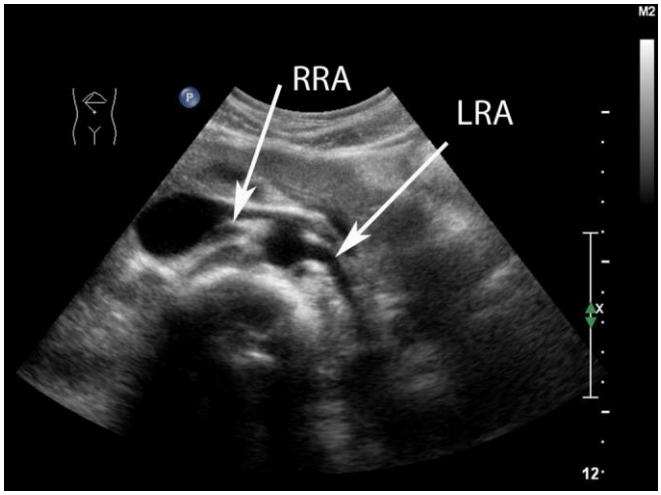

Figure 8 Ureter outlet in prone position clearly visible as tubular structure.

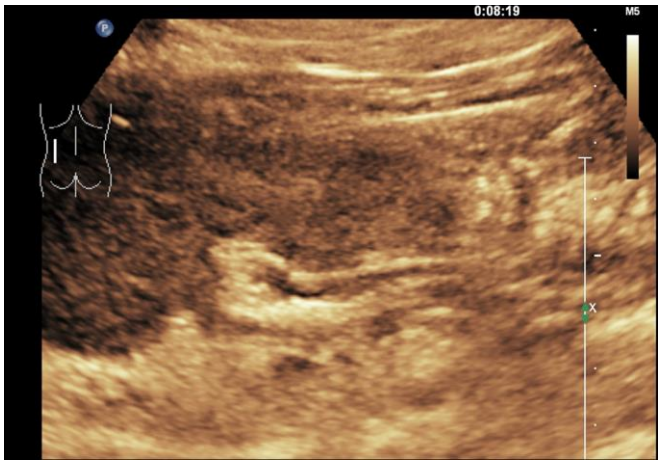

Figure 9 A renal lobule includes a single pyramid surrounded by the cortex.

Figure 10 Two adjacent lobules of a calf kidney. The lighter kidney cortex and darker pyramids are clearly visible.

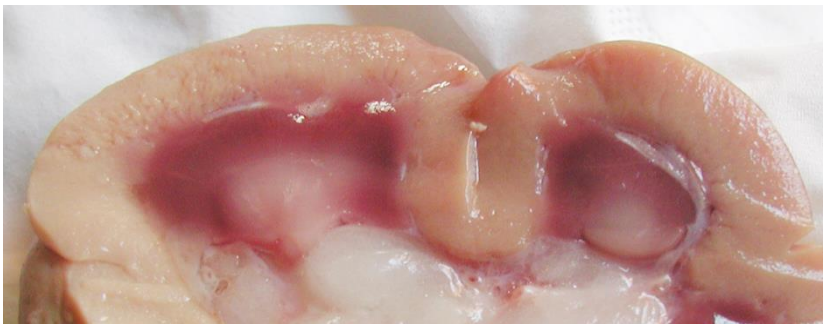

Figure 11 Lobulation, areas of renal lobule fusion are easily recognisable, especially in children.

Figure 12 Foetal lobulation in an 8-year-old child.

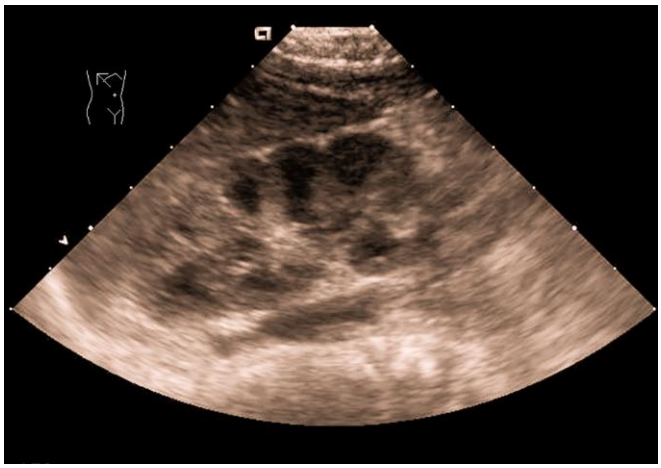

Normal findings

Size

The normal kidney measurements ([1]) are as follows:

Length (A): 9–13cm (measured in longitudinal section)

Width (B): 4–6cm (measured in cross-section)

Depth (C): 4–6cm (measured in cross-section)

Using the ellipsoid formula, the kidney volume is calculated by:

Volume in millilitres = A × B × C × (π/6)

Normal kidney volume is 90–170ml/1.73m^2. Correct measurement of the kidney volume should involve both the longitudinal- and cross-axis of the kidney [(1,2)]. Kidneys with a volume greater than 200ml/1.73m^2 BSA are enlarged and kidneys with a volume under 80ml/1.73m^2 BSA are shrunken [(1, 2)].

Parenchymal and cortical thickness

The parenchymal thickness is measured from the tip of the renal pyramid to the surface of the kidney [(2)]. Normal parenchymal thickness is 14–18mm. Parenchymal thickness can be useful but the measurement should always be carried out in the same place, *i.e*. at the same pyramides [Figure 13]. This is particularly important while monitoring a transplanted kidney, but should also be taken into account when assessing chronically diffuse diseases of the parenchyma. The cortical thickness is measured from the tip of renal pyramid to the kidney cortex surface [Figure 13]. The normal cortical thickness is 8–10mm. The cortex narrows in chronic diseases of the parenchyma and is associated with kidney insufficiency. As a result cortical thickness correlates with the degree of the kidney insufficiency [(3, 4)].

Figure 13 Measurement of parenchymal (P) and cortical (C) thickness.

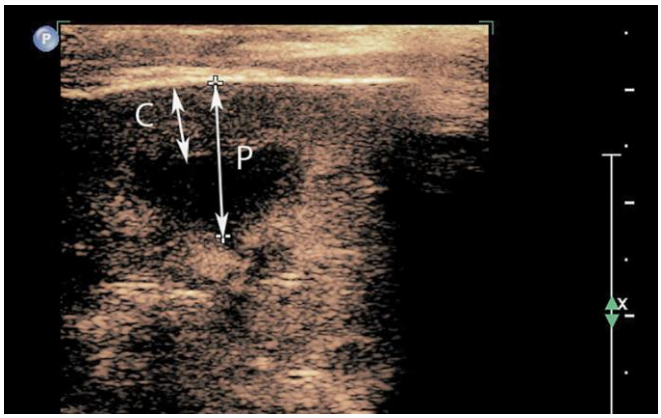

The vascular supply of the kidneys is divided into five segments the upper pole, lower pole, upper anterior, lower anterior and posterior segment. In only 60% of the population will all 5 segments originate from a single renal artery. In 8% the upper pole artery originates directly from the aorta, in 6% the lower pole artery and in 5% both pole arteries. Segment arteries divide themselves shortly before entering the kidney parenchyma. First, they give rise to the interlobar arteries then branch into the arch arteries. Further divisions of the arch arteries consist of the vasa recta leading into the renal medulla and the interlobular arteries leading into the kidney cortex.

Examination technique

The patient is first examined supine. The longitudinal axis is looked for along the edge-cut, a section which runs in a dorsal-cranial to ventral-caudal direction and in a medial cranial to caudal lateral direction. The kidney is first measured in the longitudinal plane and then in the short-axis and cross-section. The ribs can sometimes obstruct a clean cross-section. If this occurs, it is recommended the examiner finds a space between the ribs and asks the patient to breathe deeply. The whole kidney can then be examined properly and in detail. The kidney sinus is usually easily examined when the patient (either child or adult) is in the prone position. This position is usually successful for the identification of the renal pelvis and the outlet of the ureter. The kidneys can be positioned quite high and the left kidney can be subphrenic. In these cases, examination in a standing position is usually successful. This can

lead to the observation of a floating kidney (the kidney moves >5cm while standing). It is important to observe the respiratory displacement of the kidney and to compare it with the respiratory displacement of the liver (and the spleen on the left side) and the psoas muscle. Single focal space demands can then be distinguished from each other, *e.g.* cysts in kidney or spleen. A lack of displacement in comparison with the psoas muscle suggests a perinephric abscess or infiltration of the kidney by a retroperitoneal tumour.

To assess renal perfusion, a spectral analysis of the kidney parenchymal artery is obtained while the patient lies in prone [Figure 14]. Spectral curves are evaluated from arteries at the point where they are about to dip into the kidney parenchyma. Renal arteries and veins are assessed with the patient in supine position. Outlets of the renal arteries can be observed in the longitudinal axis [Figure 15–16] as well as in cross-section [Figure 8]. In cross-section, the entire length of the arteries can be seen on colour duplex ultrasonography (CDUS). Spectral analysis can be derived from a cross-section as well as in the longitudinal axis.

Figure 14 Spectral curves from interlobar artery (representing renal parenchyma).

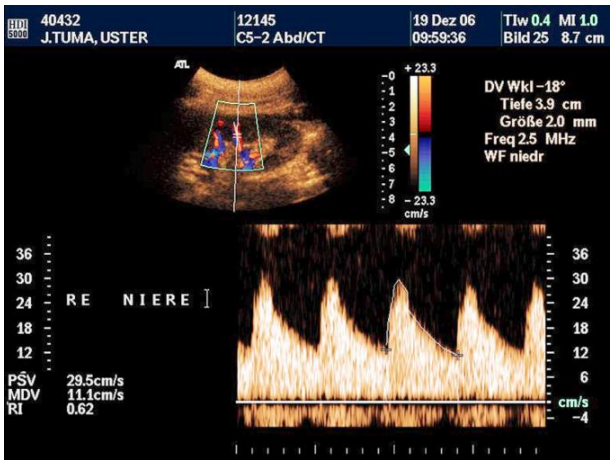

Figure 15 Longitudinal axis for renal artery outlets.

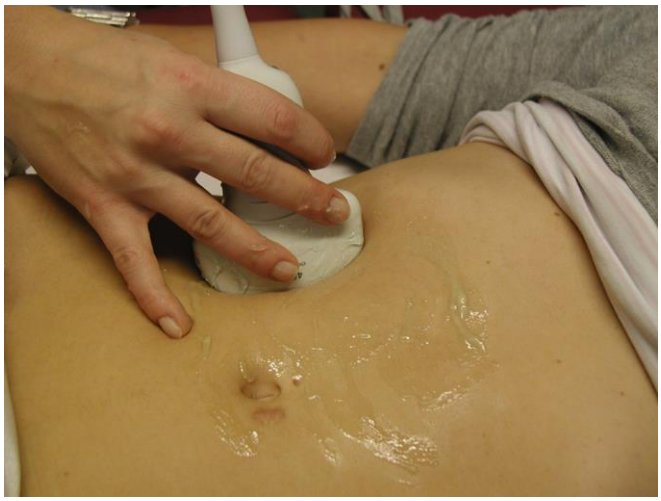

Figure 16 Longitudinal axis for renal artery outlets. Left renal artery dorsal, right ventral.

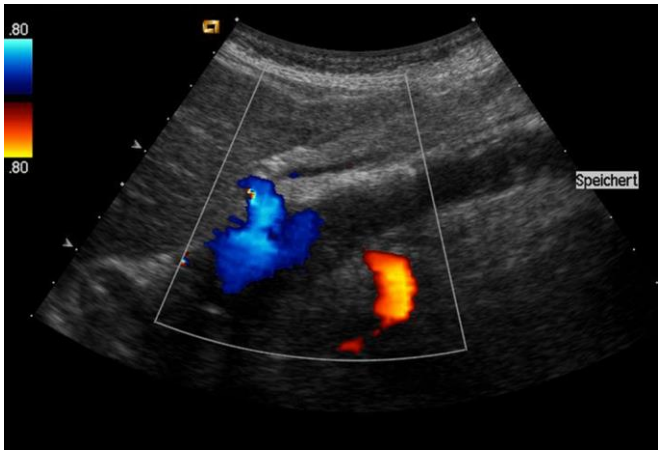

Sonographic assessment criteria

Deviation from the normal kidney shape can be used on its own or in combination with other criteria to assess pathological state. Position and form, size, contour, echo-pattern, architecture and perfusion should all be considered.

Position and shape

Owing to its complex genesis, the kidney can show many normal variations. They can be ectopic with abnormal localisations (*e.g.* pelvis kidney) or an anomaly of rotation *e.g.* ventrally-directed kidney pelvis [Figure 17]. An altered kidney form can be seen in various fusion anomalies (*e.g.* horseshoe kidney, cake kidney, etc.).

Figure 17 (a) Normal and (b) malrotated right kidney in the short axis.

Size

During acute disease of the kidney (*e.g.* acute glomerulonephritis or acute pyelonephritis) the main observation is a general enlargement of the kidney's size (length >14cm, volume >200ml/1.73m^2 BSA). However, during chronic diseases (*e.g.* chronic glomerulonephritis or pyelonephritis) the kidney is diminished (length <9 cm, volume <80ml/1.73m^2 BSA). Cortical thickness correlates with the degree of kidney insufficiency [(1).

Contour

As part of the normal variation of lobulation [Figure 11], the usually smooth contour is characterised by a wavy outline with fine drafts. These are the traces of the fusion of single lobule. Lobulation is often seen in small children and babies, rarely in adults and occasionally

in adult patients who suffer from chronic kidney disease. Junction fusion defects are sometimes observed between individual lobules [Figure 18].

Like junction fusion defects and lobulation, vascular scars are located between the renal pyramids. Vascular scars are wedge-shaped and mostly acute-angled defects of the contour [Figure 19]. In contrast, pyelonephritic scars shows a flat and concave outline. In the epicenter of the scar lies the renal pyramid [(5)]. This is caused by shrinkage in the single renal lobule [Figure 20].

Figure 18 Junction fusion defect.

Figure 19 Vascular scar.

Figure 20 Pyelonephritic scar.

Echo-pattern

The echo-pattern of the normal kidney is fine-grained and homogeneous. In adults the kidney cortex shows slightly less echo than the liver and spleen. The renal pyramids are easily recognisable and very hypoechoic. The kidney cortex is a complex structure that consists of interlobular arteries, glomerular and convoluted tubules [Figure 21]. An increase of interstitial water (*e.g.* as a result of oedema, inflammation or congestion) causes the amount of interface to increase (similar to liver haemangioma) and the kidney cortex to appear richer in echo [Figure 22]. Only when a certain water level is reached will a decrease in echo in the cortex be seen [Figure 23]. This can be observed in acute right heart failure or severe pyelonephritis.

In contrast to the renal cortex, the medullary pyramids contain parallel tubular structures, which have little influence on sonographic behaviour with changes in interstitial water. Therefore, the sonographer should be aware that there are many chronic and acute diseases of the kidney parenchyma, which are characterised by a more intense echo in the cortex of the kidney and easily identified renal pyramids.

Another modification is an enriched echo-pattern in the renal pyramids, which in most cases is due to the storage of either calcium or uric acid [Figure 24].

Figure 21 **Renal vessels are filled with red Silastic®. Arcuate and interlobular arteries and glomeruli are visible. A micropunctured tubule (with convoluted tubules, loop of Henle and collecting duct) is filled with white Silastic®.**

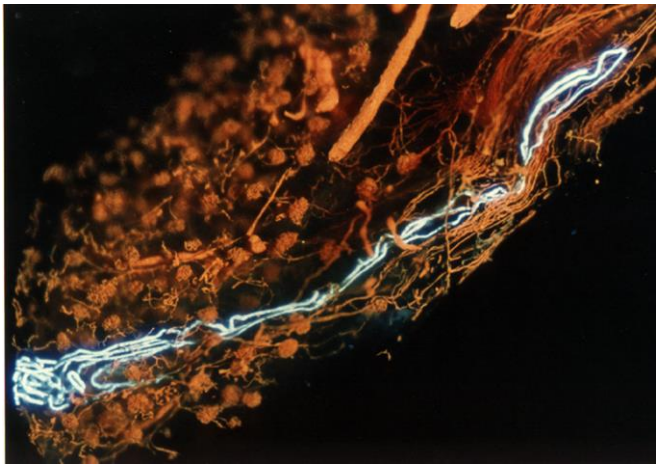

Figure 22 **Large kidney with a hyperechoic cortex.**

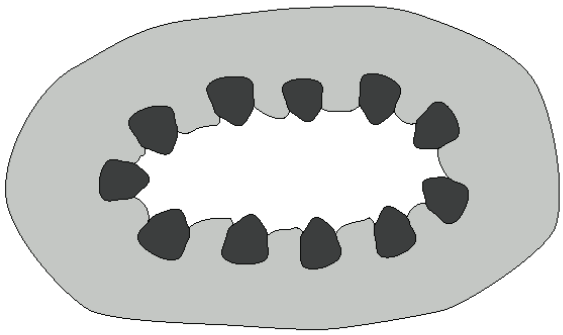

Figure 23 Large kidney with hypoechoic cortex.

Figure 24 Kidney with hyperechoic renal pyramids.

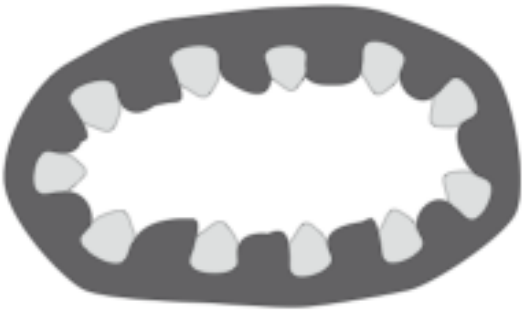

Architecture

The architecture is defined by the complex outer structure of the kidney. Any deviations from the normal architecture create a set of modifications, which cannot be described by the above criteria. In polycystic kidney disease (PCKD) or advanced chronic pyelonephritis, the generalised destruction of normal architecture is usually observed. As a result of the destroyed architecture, it is possible to recognise neoplastic modifications.

Perfusion

Evaluation of kidney perfusion is an important sonographic criterion. It can be assessed by CDUS [Figure 14], power wave Doppler sonography (PWDS), spectral analysis and contrast-enhanced ultrasound (CEUS). PWDS provides a rough estimate of the overall perfusion in the kidney parenchyma [Figure 25]; it should be spread uniformly within the parenchyma. CEUS is a more subtle assessment, which is important to assess for renal infarction [(6-9)] or acute pyelonephritic changes [Figure 26a, b]. With the values set for pulse repetition frequency (PRF) a representation of renal arteries (the segmental, interlobar, arcuate and interlobular arteries) becomes possible including a depiction of their branches [Figure 14].

Spectral analysis of the interlobar arteries allows the quantitative evaluation of kidney parenchyma perfusion. The maximum systolic velocity (V_{max}) and the minimum end-diastolic velocity (V_{min}) are detected and the resistive index (RI) ($V_{max}–V_{min}/V_{max}$) is calculated. These values play an important role in monitoring transplanted kidneys and the evaluation of diffuse renal parenchymatous disease [(10-12)]. Normal RI values lie between 0.55–0.75 and are age-dependent. For example, in an 80-year-old patient an RI of 0.75 is normal, whereas in a 30-year-old patient an RI of 0.70 is too high.

Figure 25 **Power Doppler sonography:** the whole vasculature of kidney is by this technique visible, unlike color Doppler, the angle of incidence does not matter

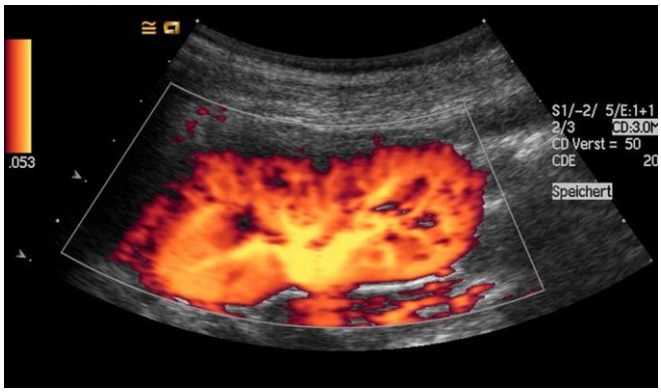

Figure 26 Patient with acute lobar pyelonephritis on an upper pole (a). Contrast-enhanced ultrasound (CEUS) in the same patient shows a visible perfusion defect 18s after contrast injection, which is typical for acute pyelonephritis (b).

a

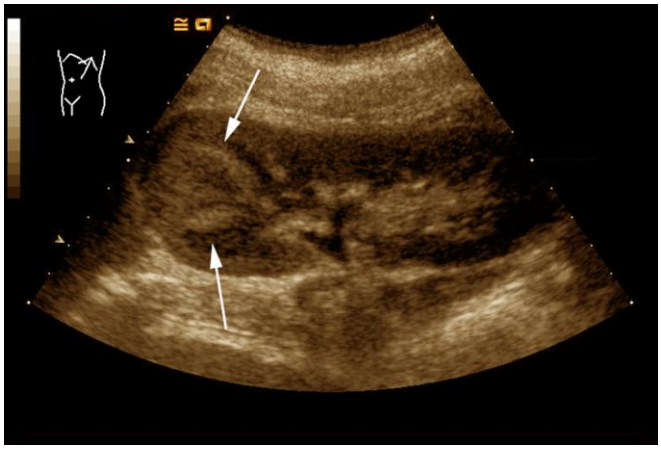

b

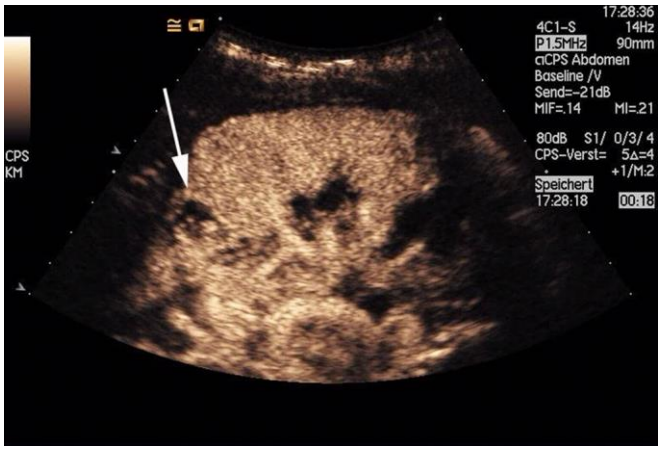

Specific sonographic findings

Variations of the kidney are classified into different groups using the sonomorphological criteria below. In a single disease, more than one criterion is considered abnormal. In such cases, the dominant criterion is used for classification and additional criteria complement the findings.

Diffuse changes of renal parenchyma

Abnormal kidney position and shape

The human kidney has a complex genesis. It develops in three steps: the pronephros, which corresponds to the primitive kidneys of fish, and performs the basic function of the glomeruli and proximal tubules. The structure of the pronephros appears in the human embryo at the fourth week of pregnancy. The structure never transgresses the rudimentary tubular stage and, unlike the fish kidney, will never produce urine. The largest part of the pronephros forms the structure for the urinary collecting system of the next kidney stage.

The development of the mesonephros can be seen towards the end of the fourth week of pregnancy, immediately caudal of the rudimentary pronephros. They consist of large and elongated organs with fully formed glomeruli. They function as interim kidneys for a period of approximately four weeks until the permanent kidneys are fully developed. The tubules of the mesonephros open in the Wolffian duct, which is the caudal continuation of the pronephros duct and distally ends in the cloaca. While the mesonephros regresses towards the end of the first trimester, some of the tubules persist and develop into the efferent ducts of the epididymis. The development of the metanephros or the definitive kidney begins in the fifth week. After approximately four weeks the kidneys begin to function. The permanent kidney develops from two main sources: the ureteric bud and the metanephric blastema. The ureteric bud forms a protuberance of the Wolffian duct close to its connection at the cloaca. The metanephric blastema is derived from the caudal portion of the nephrogenic cord. The ureteric bud later evolves into the ureter and the extended middle section evolves into the renal pelvis. The top of the bud branches several times and evolves into the calices and the collecting duct. The ampullary end of the arch-like collecting duct develops into the glomeruli and tubules in the metanephric blastema. Each collecting duct is therefore linked to proximal and distal tubules as well as to the loop of Henle and to the glomerulus. It forms the functional unit of the kidney, *i.e.* the nephron. The development of the glomeruli is already complete by the 32nd week of pregnancy when the final number of glomeruli is reached. In cases of disturbed development, the ureteric bud plays a central role because of its impact on the complex modifications to the architecture of the kidney. In

some cases, a disturbance of the fusion processes of a single renal lobule can occur. This leads to a series of anomalies to the structure, position and form of the kidneys [(13)].

Agenesis

If there is no interaction between the ureteric bud and metanephric blastema, the kidney will not develop on that side. This will also happen if the ureters and collecting duct are missing and there are abnormalities in the area of the epididymis. If the kidney is not found in the typical position, it can be assumed agenesis has occurred.

Aplasia

In the case of a faulty interaction between the ureteric bud and metanephric blastema kidney aplasia can occur. Sometimes, minimal traces of the kidney (only a few millimetres) can be seen and, occasionally, anechoic tubular malformations in the area of the blind-ending ureters can appear [Figure 27].

Figure 27 Tubular anechoic ureteric malformation in case of renal aplasia: tubular Structures on the left side of bladder, blind ending.

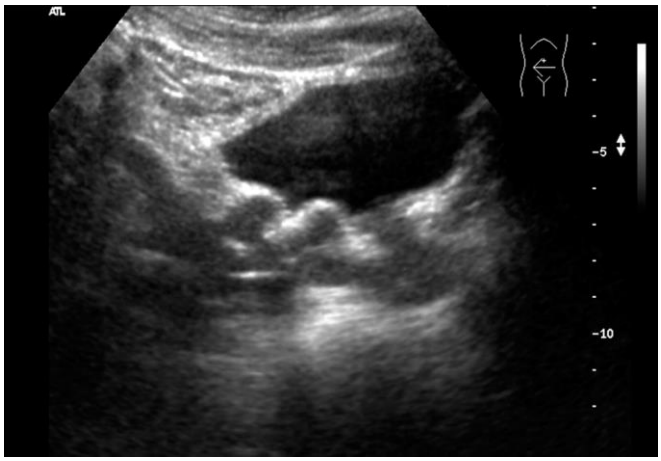

Dysplasia

A poor interaction between the ureteric bud and metanephric blastema will result in a multicystic organ with mostly degenerated tubular structures. In only a few cases will intact nephrones develop. They fulfil excretory functions, but usually this is lost shortly after birth. The multicystic dysplastic kidney (MCDK) will usually appear on only one side [Figure 28]. Sometimes only a part of the kidney will show this dysplasia.

Figure 28 Multicystic dysplastic kidney in an 8-year-old child.

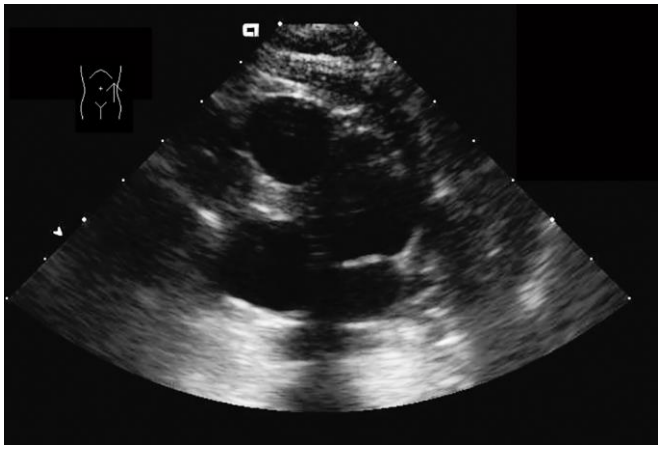

Rotation anomaly

A failed or excessive rotation sometimes occurs when the renal hilum leaves the kidney, which normally happens ventrally [Figure 17]. Anomalies of rotation are often associated with kidney dystopia.

A rotation anomaly can result in limited or unusual sections of the parenchyma that can generate images, which are easily mistaken for a solid mass.

Double kidney

In the case of a double system, a particularly long kidney can be found that usually has an incision in the parenchyma and a parenchyma bridge [Figure 29]. The demonstration of two arteries and ureters is proof of a double kidney.

Figure 29 Double kidney with two renal arteries.

Sigmoid kidney

The sigmoid kidney is another form of the double kidney. The caudal part is malrotated and the other part shows an inconspicuous renal hilum [Figure 30].

Figure 30 Sigmoid kidney with a normal upper and malrotated caudal part.

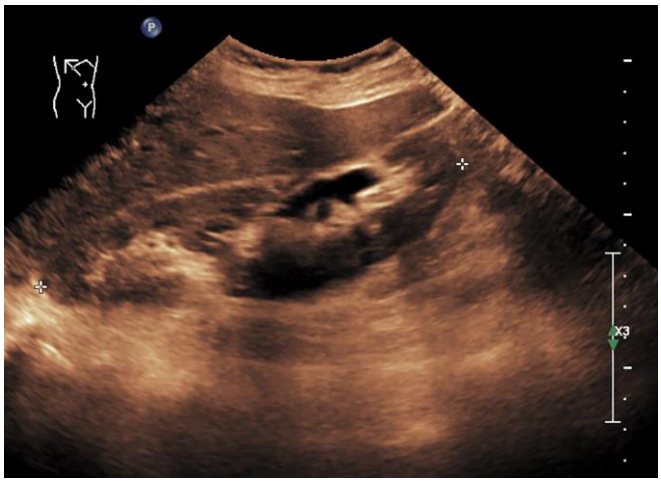

Horseshoe kidney

In a horseshoe kidney, the kidneys are fused at the lower pole and the parenchymal bridge is located in front of the aorta and should not be confused with a solid mass [Figure 31].

Figure 31 Horseshoe kidney.

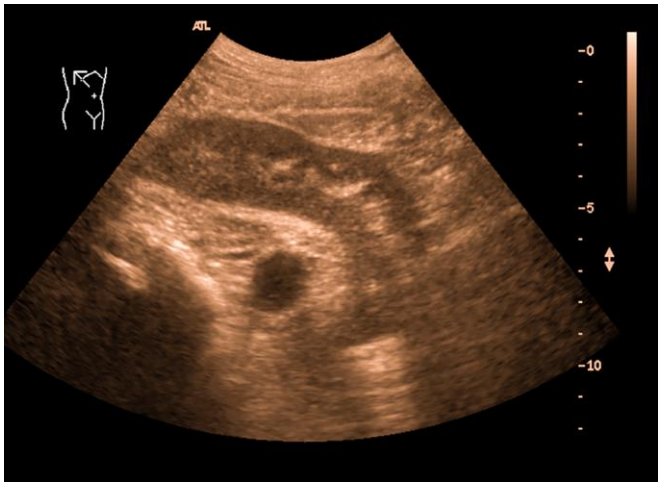

Pancake kidney

The cake kidney is located in front of the sacrum. The kidney is completely merged with two ureters [Figure 32].

Figure 32 Pancake kidney.

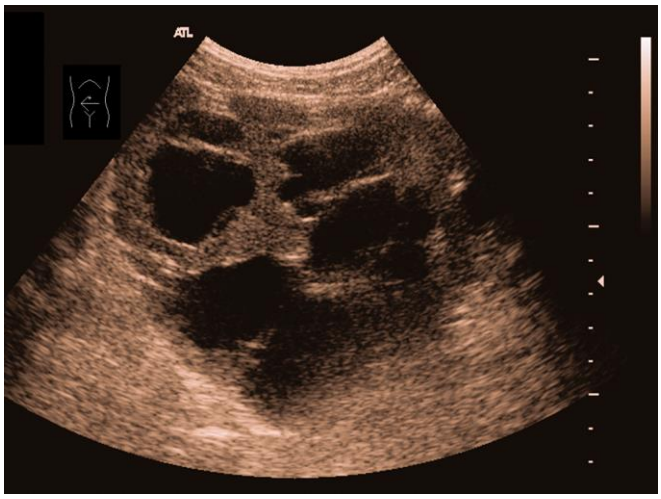

Hypoplastic kidney

The hypoplastic kidney consists of an overall reduced, but otherwise normally developed kidney. In most cases, the parenchyma is less than 13mm thick and the total volume is less than 80ml/1.73m^2 BSA.

Ectopic kidney

Ectopic kidneys are kidneys that are not in their normal position. Failure to show the kidney in a normal position does not necessarily mean aplasia or agenesis. The kidneys should be looked for elsewhere in the retroperitoneum. For example, the pelvic kidney is found deep in the abdomen. These ectopic kidneys are often supplied by the iliac artery (similar to a transplanted kidney).

Nephroptosis

This is a dynamic position anomaly. When the patient is in a lying position the kidney is in its normal location, but in standing it can drops by more than 5cm.

Enlarged kidneys

Kidneys count as enlarged when their longitudinal diameter is more than 14cm or has a volume of over 200ml/1.73m^2 BSA. The width of the parenchyma is usually over 18mm and the cortical width over 10mm. Enlarged kidneys are further sub-divided into kidneys with normal cortex echo-intensity, with hyperechoic cortex and with hypoechoic cortex [(14)].

Enlarged kidneys with echo-normal cortex

A compensatory renal hypertrophy or a solitary kidney leads to an increase in volume and parenchymal thickness, which in most cases exceeds 20mm. The cortex is usually echo-normal or slightly hyperechoic. The renal pyramids are normally inconspicuous in these cases.

Enlarged kidneys with hyperechoic cortex

The identification of an enlarged kidney with a hyperechoic cortex and conspicuous medullary pyramids is non-specific [(15-17)]. The increase of echogenicity is caused by an interstitial oedema and/or by infiltrates [(18, 19)]. Often, these are acute diseases. Normalisation of the kidney size and the echogenicity of the kidney cortex is observed after successful treatment or they resolve on their own (acute and quickly progressive glomerulonephritis, acute interstitial nephritis or acute pyelonephritis). In cases of bilateral disease normalisation of kidney function occurs. The findings are non-specific and further assignment of the disease is only possible by the following clinical criteria:

- acute nephritis;
- nephrotic syndrome;
- acute renal failure;
- acute pyelonephritis;
- infiltrative nephropathies
- acute urinary tract obstruction.

Acute nephritis

Acute nephritis syndrome is defined clinically by glomerular haematuria, erythrocyte casts, hypertension, renal failure and/or oedema. This could be caused by acute glomerulonephritis or systemic disease (polyarteritis nodosa, Wegener's granulomatosis, etc.) The definitive diagnosis of acute glomerulonephritis is made through a renal biopsy [Figure 33]. Kidneys with acute nephritis show enlargement, a hyperechoic cortex and hypoechoic clearly visible renal pyramids [(20)].

Figure 33 Acute glomerulonephritis (immunoglobin A nephropathy).

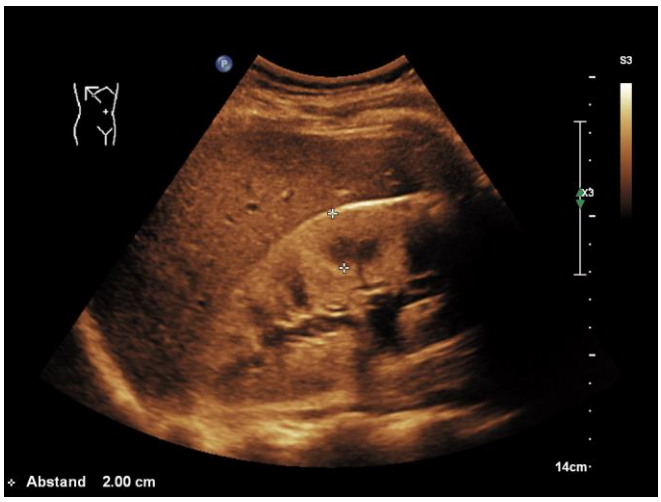

Nephrotic syndrome

The nephrotic syndrome is defined by proteinuria of greater than 3.5g/24h/1.73m^2 BSA. The kidney cortex is hyperechoic. In most cases there is little enlargement and instead they are surrounded by an anechoic sharp edge due to edema caused by hypoproteinaemia. Precise classification of the disease responsible is only possible after renal biopsy.

Diabetic nephropathy

Diabetic nephropathy can also cause nephrotic syndrome. Even in the early stages kidney enlargement can be seen. Initially the kidney cortex is discrete, but it becomes more hyperechoic. The kidney can be enlarged or of normal size in the dialysis stage even with increasing renal failure [Figure 34].

Figure 34 Diabetic nephropathy with nephrotic syndrome. Plasma-creatinine 190 µmol/l.

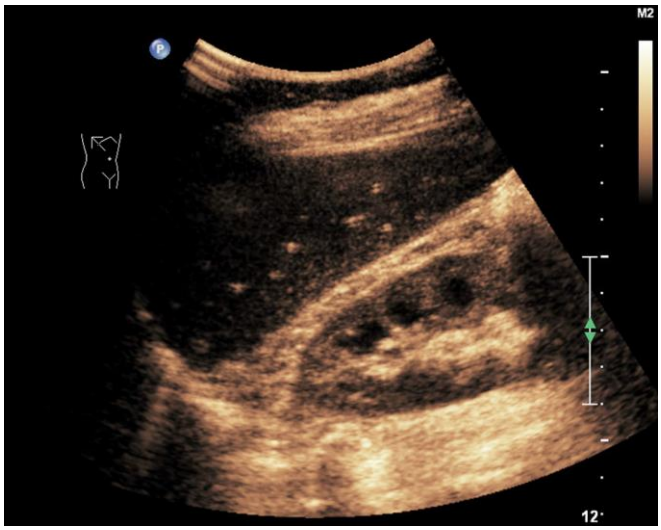

Acute renal failure

Acute renal failure is defined as less than 3 months. There will be no renal anaemia and the level of serum creatinine will increase weekly or even daily.

Acute interstitial nephritis

Acute interstitial nephritis is a disease arising from a reaction to various medications (*e.g.* penicillin, non-steroidal anti-inflammatory drugs, etc.) or infections (*e.g.* leptospirosis). Its sonomorphology is characterised by enlarged kidneys, a hyperechoic cortex and clearly visible hypoechoic renal pyramids [(14)]. This disease is assumed on the basis of a characteristic case history, its progress, sonomorphology and evidence of eosinophil leukocytes in the urine; although a definitive diagnosis can only be given on renal biopsy.

Acute tubular necrosis

If acute tubular necrosis emerges during circulatory shock, the kidneys do not usually show any enlargement and the cortex is not any more echoic than normal. In many cases, the kidneys are inconspicuous on ultrasound. This differs from a crash kidney, in which inhomogeneous, hyperechoic and hypoechoic areas of the cortex and an overall enlargement of the kidney are found. Similar results are also seen in cases of toxicity-caused tubular necrosis, *e.g.* aminoglycosides [(21)].

Acute pyelonephritis

Severe cases of pyelonephritis show a diffuse enlargement of the organ with an hyperechoic cortex and prominent hypoechoic pyramids. A thickening of the renal pelvis wall [(22)] is detectable in most cases (≥3 mm; normal is <2mm). Owing to a disturbance in renal pelvis motor activity, a slight dilatation can be observed [Figure 35]. The typical findings of fever, lumbar pain and high C-reactive protein make acute pyelonephritis likely. The distinction between an acute pyelonephritis and a simple urinary tract infection is usually made on CEUS [(8)] combined with clinical presentation. The less perfused areas in the kidney parenchyma are shown and allow a diagnosis of pyelonephritis to be made, similar to MRI [(23)]. Pyelonephritis can lead to focal modifications where often only a single lobulus is affected.

Figure 35 Acute pyelonephritis in a 18-year-old female. The cortex and medulla are hyperechoic and the pelvis wall is thickened (3.8 mm).

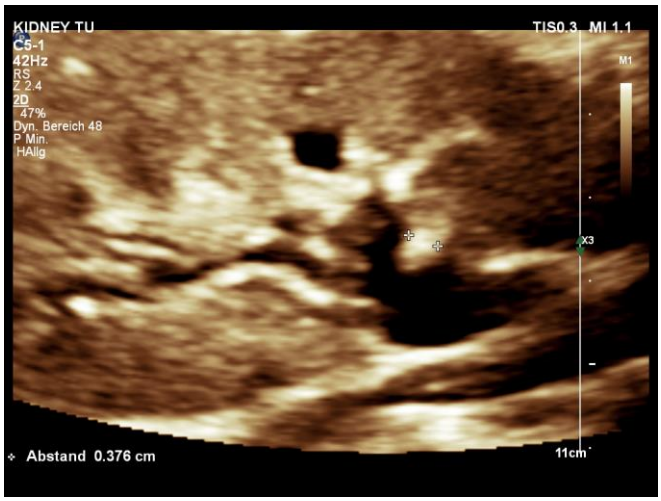

Infiltrative nephropathies

The category of infiltrative nephropathies includes diseases that show large hyperechoic kidneys, such as storage diseases, lymphomas and leukaemias. Of all storage diseases, amyloidosis is the most clinically relevant and manifests as nephrotic syndrome. The echo compaction of the kidney cortex and the kidney cortex itself is very strong in these cases.

The whole kidney is diffusely infiltrated [(24)] by amyloid [Figure 36]. Niemann-Pick disease is a very rare lipid storage disorder and has a similar appearance. A diffuse infiltration of the kidney by non-Hodgkin‘s lymphoma or leukaemia can also result in the manifestation of a large kidney with hyperechoic cortex and even more echoic and less prominent renal pyramids [(25)].

Figure 36 Amyloidosis with nephrotic syndrome and normal creatinine. Large kidney with hyperechoic cortex.

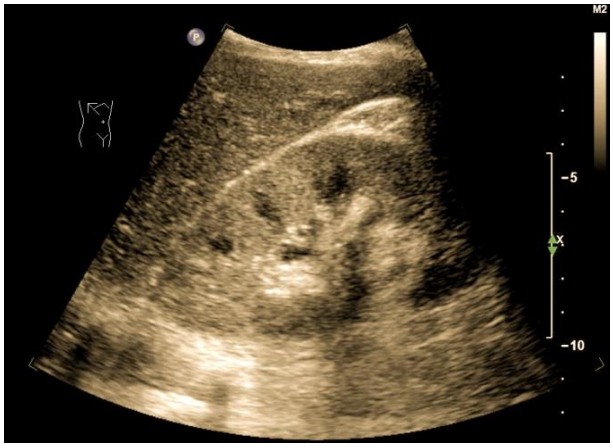

Acute urinary tract obstruction

In cases of a renal colic with an acute urinary obstruction, an enlargement of the affected kidney and a hyperechoic cortex can be observed [Figure 37]. The kidney pelvis then becomes extended and at this stage a significantly raised RI is seen (increased RI≥0.10 on the affected side).

Figure 37 Acute urinary tract obstruction in very early stage. No hydronephrosis but enlarged kidney with hyperechoic cortex.

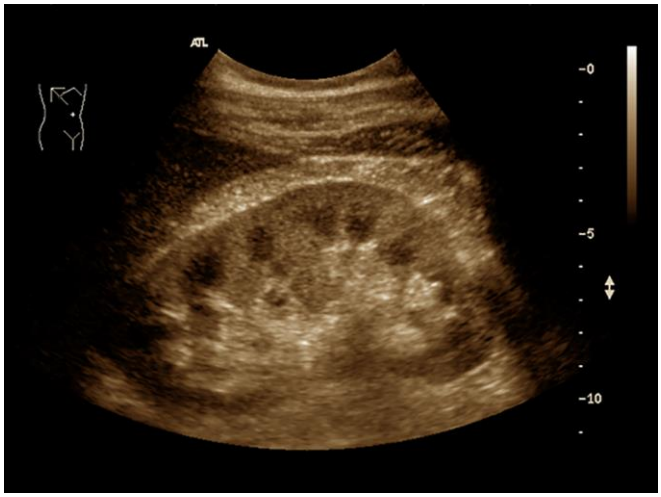

Enlarged kidneys with hypoechoic cortex

This has been observed during cases of severe acute right heart failure, renal vein thrombosis and in Hantavirus infection. Attenuated echogenicity of the cortex with an overall enlarged kidney has been described. A part of the inflamed kidney parenchyma can also appear hypoechoic in cases of focal pyelonephritis.

Small kidneys

Small kidneys are defined as kidneys with a longitudinal diameter of less than 9cm or a kidney volume below 80ml/1.73m^2 BSA. Small kidneys occur in kidney hypoplasia, vascular diseases of the kidney and in cases of chronic disease of the kidney parenchyma. In the same way as enlarged kidneys, small kidneys are further sub-divided into kidneys with normal cortex echo-intensity hyperechoic cortex or hypoechoic cortex [(14)].

Small kidney with normal cortex echo-intensity

Kidney hypoplasia

Hypoplasia is the result of a disturbance to the kidney's development and is characterised by a reduced organ size and an otherwise inconspicuous appearance [Figure 38]. A combination of hypoplasia with dystopia and malrotation can occur.

Figure 38 Hypoplastic small kidney, otherwise normal architecture.

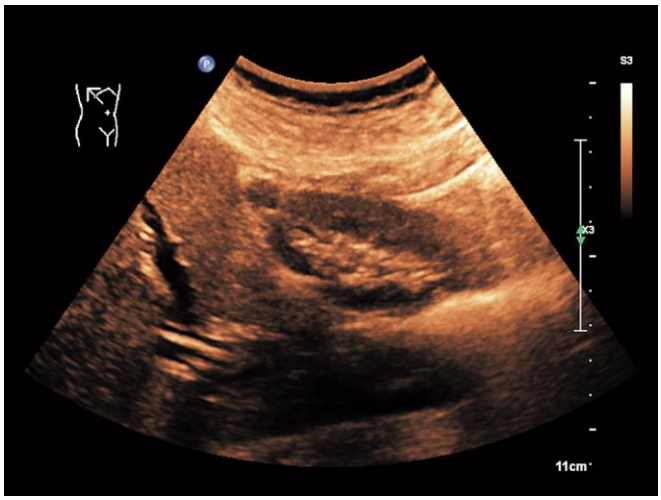

Nephrosclerosis

Kidneys of patients suffering from general arteriosclerosis and/or chronic hypertension are normal size or only slightly smaller. They have an inconspicuous echogenicity of the kidney cortex and, often, characteristic vascular scars can be seen. The RI increases to a value of 0.8 or higher. The high value corresponds with a rapid progression towards renal failure [Figure 39]. As a result of the vascular damage, there is also significant narrowing of whole parts of the kidney parenchyma [Figure 40].

Figure 39 Nephrosclerosis with high resistive index (0.81).

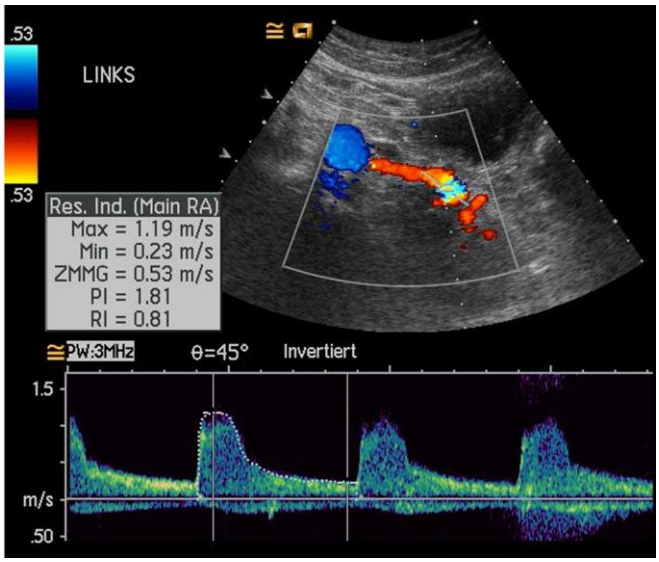

Figure 40 Nephrosclerosis with narrowing of huge part of parenchyma.

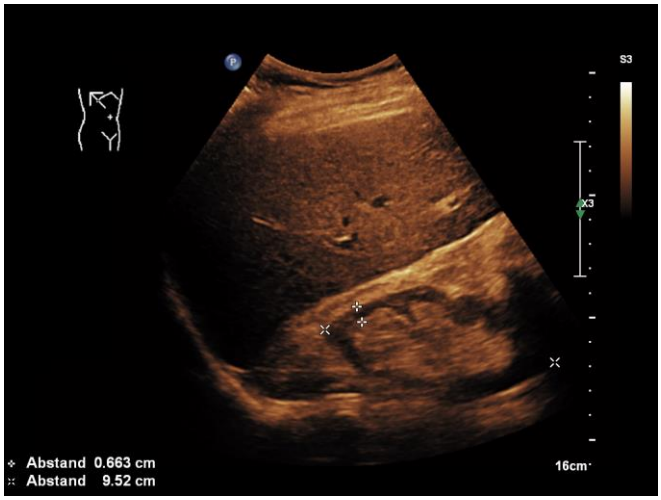

Small kidney with hyperechoic cortex

It makes sense to combine further clinical features and syndromes into the differential diagnoses. If the kidney is small on both sides, then chronic renal failure normally appears. However, this is not the case for one-sided disease (*e.g.* pyelonephritis). Chronic renal failure

is characterised by being present for the 3 months, renal anaemia and/or renal osteopathy. Small kidneys on both sides is characteristic of chronic renal failure [Figure 41].

Figure 41 Small kidney with hyperechoic cortex.

Chronic glomerulonephritis and chronic non-destructive interstitial nephritis

Sonomorphology in both cases appears very similar. An hyperechoic cortex, prominent renal pyramids, fine granular contour of the kidney and a well-preserved architecture can be observed [Figure 42]. Again, obvious lobulation is apparent in many cases. A definitive diagnosis can only be made in a clinical context (*e.g.* glomerular erythrocyturia during chronic glomerulonephritis) or on the basis of renal biopsy [(20, 26)].

Figure 42 Chronic glomerulonephitis.

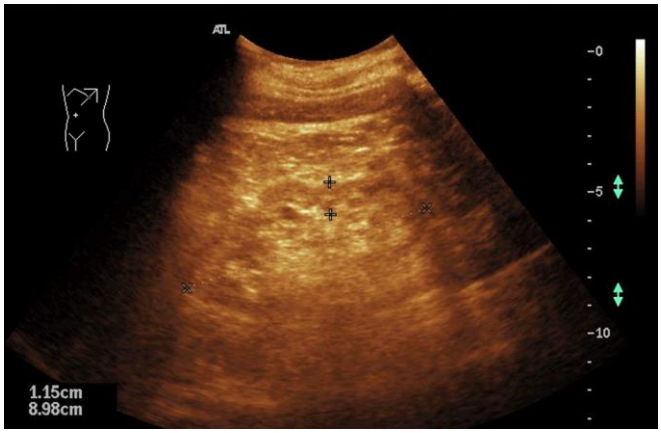

Primary oxalosis and hereditary hyperoxaluria

The renal cortex and medullary pyramids are extremely hyperechoic in both cases. Oxalate crystals are diffusely distributed in the parenchyma and normal parenchymal structures are no longer recognisable [Figure 43].

Figure 43 Hereditary hyperoxaluria.

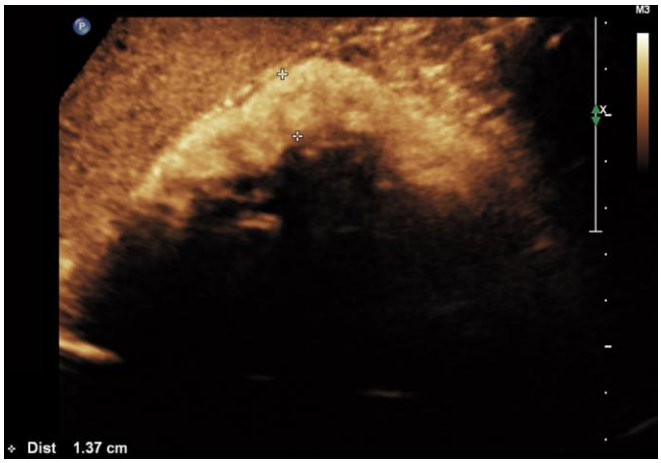

Chronic pyelonephritis

This is often a unilateral disease, but can occur on both sides and lead to chronic renal failure. Observations include typical pyelonephritic scar, a hyperechoic cortex and disturbed architecture. Large areas of the kidneys become shrunken and others are locally hypertrophic [Figure 44]. The combination of urinary tract obstruction and infection results in a rare case of pyelonephritis called xanthogranulomatous pyelonephritis, which mimics tumourous diseases [(27)]. Renal tuberculosis often shows parenchymal scarring, calcifications, congestion and stenosis in the urinary collection system.

Figure 44 Chronic pyelonephritis with an irregular destructed kidney.

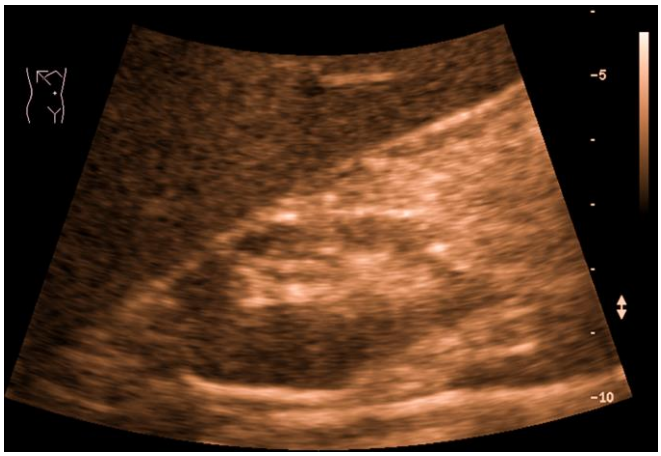

End-stage renal disease

All chronic diseases can lead to a barely recognisable and shrunken kidney. Even with histology, with end-stage renal disease (ESRD), it is difficult to differentiate between chronic pyelonephritis and chronic glomerulonephritis. Tuberculous pyonephrosis with extensive caseous necrosis is known to occur at end-stage tuberculosis and there are normally no traces of a regular structure.

Small kidneys with hypoechoic cortex

Renal artery stenosis

Renal artery stenosis can lead to a hypoperfusion of the whole organ and atrophy of tubules, which move closer together. There are no infiltrates or oedema. The kidney cortex seems more hypoechoic [Figure 45 and 46a-c]. In patients with hypertension, a systematic search for renal artery stenosis is helpful.

Figure 45 Small kidney with hypoechoic cortex with stenosis of renal artery.

Figure 46 Small kidney with hypoechoic cortex with stenosis of renal artery (a). Same case, exit of the right renal artery with Vmax 254 cm/sec (b). Same case, renal artery near the hilum with typical low poststenotic RI of 0.43 (c).

a

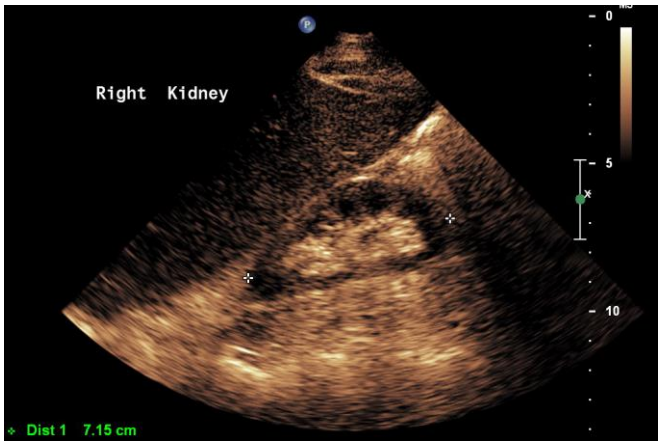

b

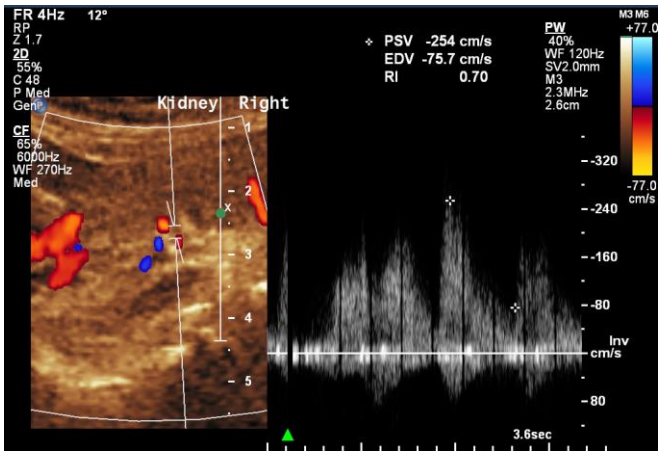

c

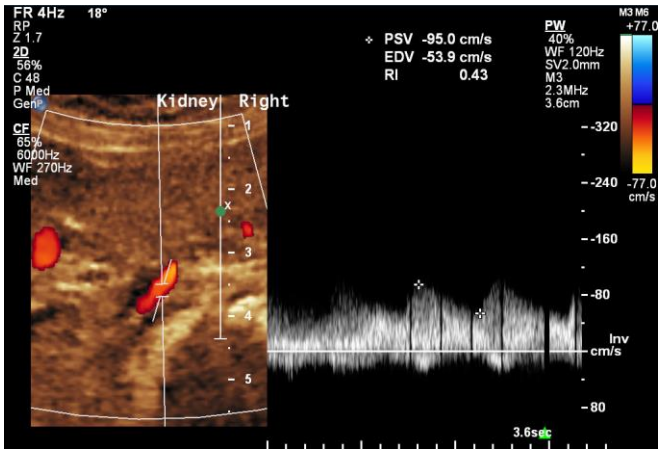

Kidney contour changes

The normal kidney contour is smooth. It has the regular demarcation of a bean-like organ. There are typical deviations of this contour [(5)] in the numerous normal variations and diseases.

Dromedary hump

A hump of the outline outwards is the so-called Dromedary hump and is a variation of the left kidney only. It is presumed that, due to the large amount of space caudal of the spleen, the kidney is able to grow during organogenesis, which is not possible on the other side where the kidney lies close to the large liver.

Lobulation

The kidney originates from the merging of 12–15 lobuli. During childhood and occasionally in adults, this fusion is incomplete. This incomplete fusion or merging is called lobulation. Each renal pyramid near it forms a lobulated kidney contour. The renal pyramid always shows in the epicentre of the lobulus and the neighbouring lobuli form an arch with each other. Sometimes, fusion grooves appear slightly deeper, but even with depth a sharp angle forms and the hump is still clearly recognisable [Figure 12].

Vascular scar

In contrast to lobulation, vascular scars originate from the arterial flow circuit of renal arterial branches, which leads to infarction of the tissue. The vascular scar is usually triangular, an acute angle-shaped defect, but sometimes it can be trapezoid [Figure 19, 47]. Trapezoid scars often lie between single renal pyramids, where the interlobar arteries plunge into the parenchyma. These scars are often found in patients who suffer from severe arteriosclerosis, or emboli from endocarditis or atrial fibrillation. These scars can often be seen in cases of chronic hypertension.

Figure 47 Vascular scar (arrow).

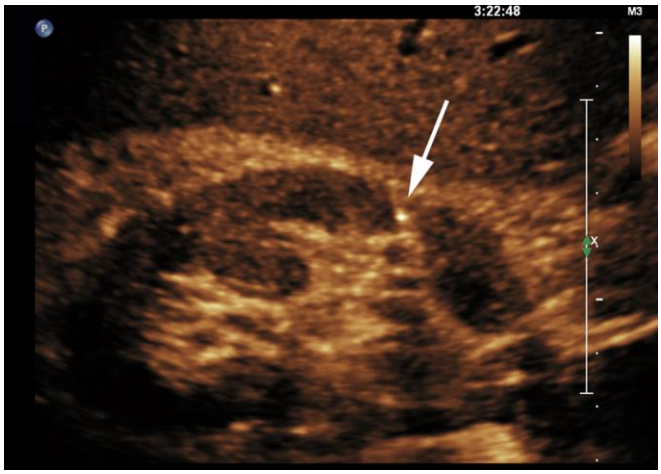

Pyelonephritic scar

The pyelonephritic scar is part of a chronic inflammatory change, which takes place in one or more lobuli. The affected kidney cortex, which is located just above a renal pyramid, shrinks and, in most cases, it is more hyperechoic than the surrounding cortex. Under these circumstances, a shallow and concave scar with a renal pyramid at its epicentre develops [Figure 20, 48a-b].

Figure 48 Pyelonephritic scar is concave, in the epicentre is the renal pyramid, surrounding parenchyma more echogenic and narrowed (a). Pyelonephritic scars in chronic disease with narrowed parenchyma, calcified necrotic papillae and enlarged renal calyces (b).

a

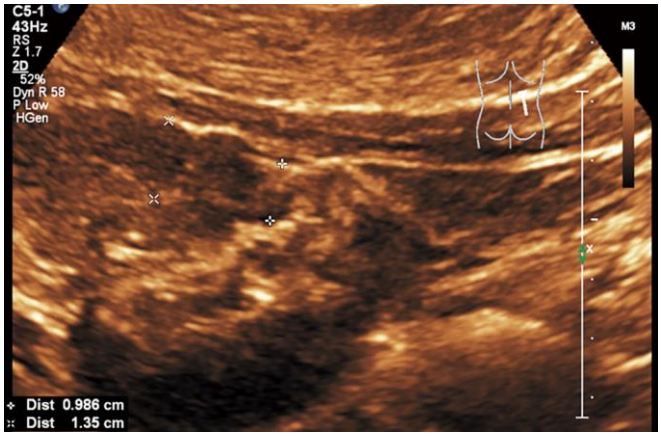

b

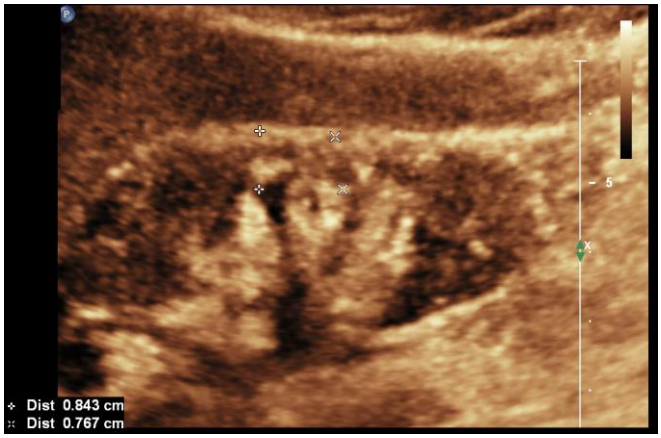

Kidney with abnormal echo-pattern

The normal echo-pattern of the kidney is homogeneous and the renal pyramid is easily recognisable as triangle-shaped and nearly anechoic formation. The peak of the pyramid and the renal papilla point towards the hyperechoic renal sinus. The base is limited by arcuate arteries. The kidney cortex can be both hyperechoic and hypoechoic. Changes to the medullary pyramids can also occur.

Kidney with hypoechoic medullary pyramids

In cases of slight right heart failure, in patients taking diuretics and with immunoglobin A nephropathy, the medullary pyramids can seem particularly hypoechoic. After precise measurement of the kidney cortex and the medullary pyramids echogenicity before and after taking diuretics, the effect on the hypoechoic medullary pyramids becomes evident as a result of the echo densification of the cortex [(18)]. Other conditions, such as immunoglobin A nephropathy [Figure 33] or early stage transplant rejection, can also show the particularly prominent and hypoechoic medullary pyramids [(14-16, 20)].

Kidney with hyperechoic medullary pyramids

The following are a series of diseases that show the opposite of the usually common echo-pattern (medullary pyramids show less echo than the kidney cortex) [(14, 17)].

Renal failure in newborns

Newborns who have been born with a lack of oxygen show renal failure that lasts only a couple of days. Characteristically, the medullary pyramids appear hyperechoic. This is thought to be due to a breakdown of the Tamm-Horsfall protein in the collecting ducts [(28, 29)].

Medullary nephrocalcinosis

There are a variety of different conditions leading to hypercalciuria and precipitation of calcium in the medullary pyramids, such us primary hyperparathyroidism, sarcoidosis and multiple myeloma. Hyperechoic medullary pyramids are also observed in Conn’s syndrome, in some forms of Bartter syndrome [Figure 49] and during furosemide abuse. The medullary

pyramids gradually become hyperechoic, which begins on the lateral side and spreads slowly into the middle of the papilla [(30-32)].

Figure 49 Medullary nephrocalcinosis in Bartter syndrome with hyperechoic pyramids.

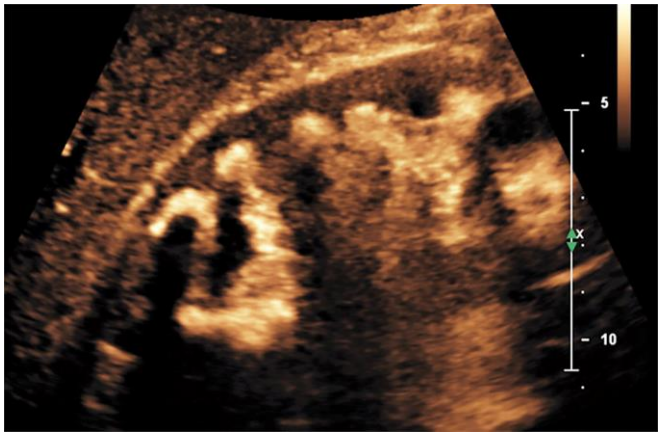

Urate nephropathy

In cases of acute urate nephropathy caused by a sudden surge of uric acid, a significant increase in volume and an echogenic kidney can be observed. These modifications are a consequence of the precipitation of uric acid crystals in the tubules, which cause urinary obstruction. Sometimes, crystallisation can be localised in the collecting ducts, particularly during long-term hyperuricosuria. Hyperechoic medullary pyramids are also seen here.

Medullary sponge kidney

Medullary sponge kidney is a congenital malformation of the collecting duct, which shows cystic extension and is often combined with distal renal tubular acidosis. The medullary pyramids are hyperechoic. Single small stones are observed inside the cystic extensions. The renal pyramids have an overall crumbly character with individual hyperechoic spots and show a very fine posterior acoustic shadow [Figure 50].

Figure 50 Medullary sponge kidney with very small stones (echogenic spots) in cystic extensions of collecting ducts (arrows).

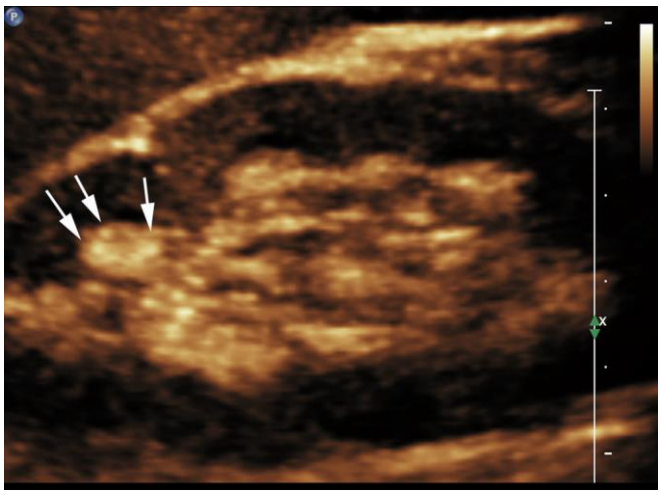

Analgesic nephropathy

As a result of phenacetin abuse, analgesic nephropathy has become a very common disease. The formation mechanism comes from capillary sclerosis in the vasa recta of the medullary pyramids, which leads to papillary necrosis at the point of the papilla [Figure 51]. During the early stages hyperechoic spots are recognisable at the point of the papillae and later almost all the medullary pyramids become calcified and necrotic. A small shrunken kidney with hyperechoic calcified medullary pyramids is found in advanced stages [(33-35)].

Figure 51 Analgesic nephropathy (early stage) with calcified tips of the papillae (arrows).

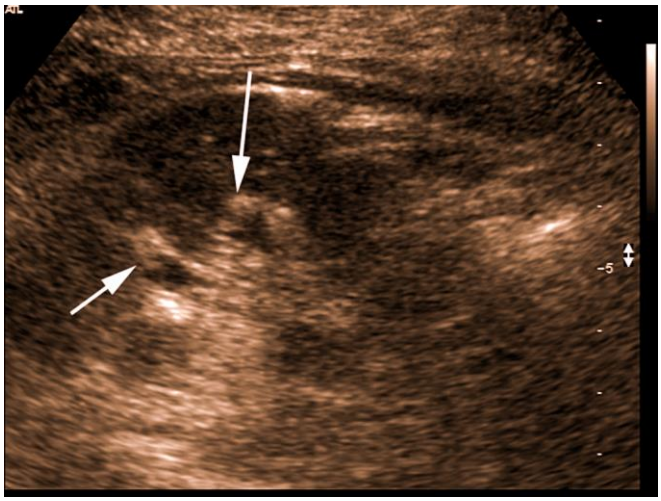

Kidney with abnormal architecture

It is necessary to be aware of the complex genesis of the human kidney in order to understand its abnormalities.

Multicystic dysplastic kidney disease

MCDK disease originates from a missing connection between the metanephros and Wolffian duct. This can take place either partially, where multicystic dysplastic focal modifications appear, or more generally where the whole kidney system shows cystic degeneration.

Polycystic kidney disease

PKD is a familial disease. The cysts form out of pre-existing tubular structures. Its appearances are classified into juvenile, autosomal recessive and adult forms. The most common type is autosomal dominant.

Autosomal recessive polycystic kidney disease

In cases of autosomal recessive polycystic kidney disease (ARPKD) there are numerous very small cysts[Figure 52]. In newborns, the appearance is reminiscent of "salt and pepper" and

can lead, in the very young to end stage renal disease (ESRD). Rarely, renal function remains into adulthood. At a later stage, multiple calcifications in the cyst walls are observed, which give the appearance of twinkling.

Figure 52 Autosomal recessive polycystic kidney disease with multiple small cysts (salt and pepper pattern) in 27-year-old female.

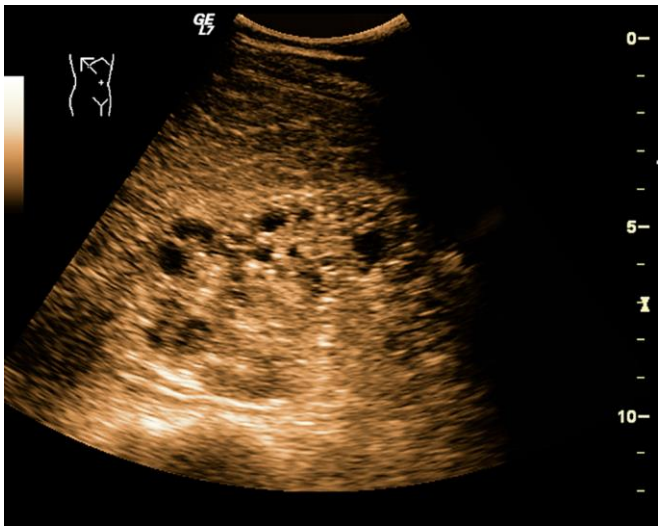

Autosomal dominant polycystic kidney disease

This variation consists of a large number of big cysts. Clinically, this disease manifests during adulthood [(36, 37)]. Numerous very small cysts are observed next to the larger cysts [Figure 53]. Many calcifications are shown by twinkling on the image. The volume of such a kidney can reach up to 1000 ml.

Figure 53 Autosomal dominant polycystic kidney disease with multiple large cysts.

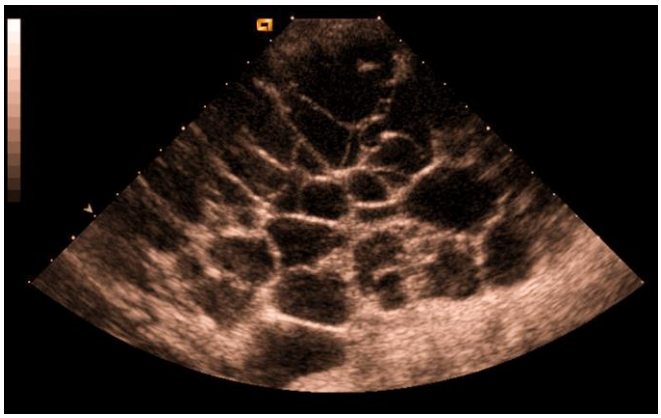

Tuberous sclerosis complex (TSC)

Is a rare genetic disorder caused by mutation of two genes TSC 1 and TSC2. There are abnormalities in many organs including skin, brain, lungs, heart, eyes, pancreas and kidney. In kidneys they are multiple angiomyolipomas in 60-80% [a] and in 20-30% kidney cysts [b].

Figure 54 Patient with TSC shows multiple hyperechoic angiomyolipomas (a) with multiple kidney cysts (b).

a

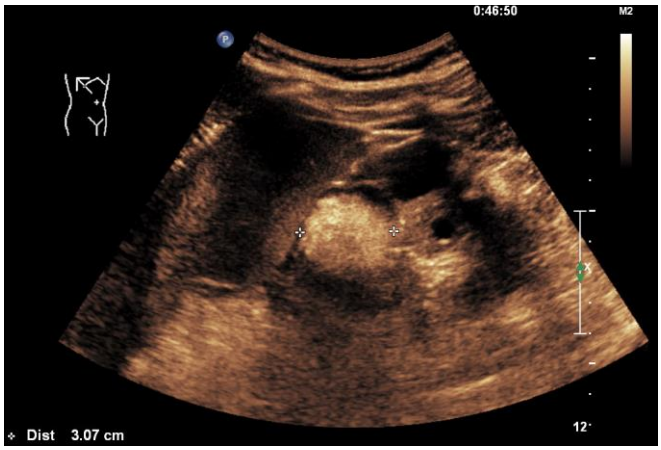

b

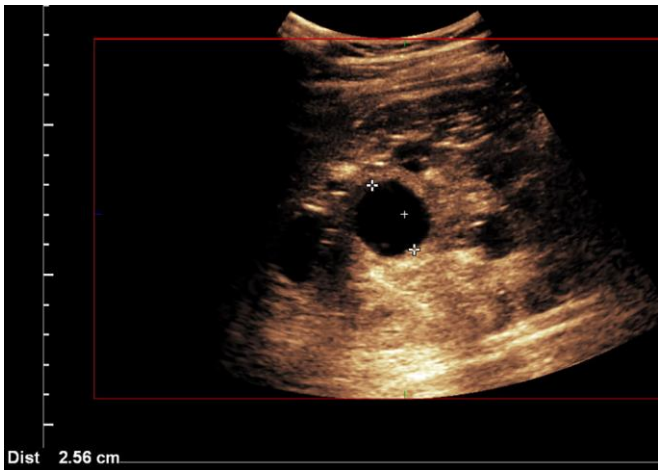

Secondary cystic degenerations with chronic renal failure

In chronic renal failure there are a number of secondary cystic degenerations, which do not have a specific cause [(38)]. The kidneys have multiple cysts, but they never reach the scale of variety or volume seen in forms of AD PKD. This degeneration is usually seen in long-term dialysis patients [Figure 55].

Figure 55 Secondary cysts in end stage renal failure patient.

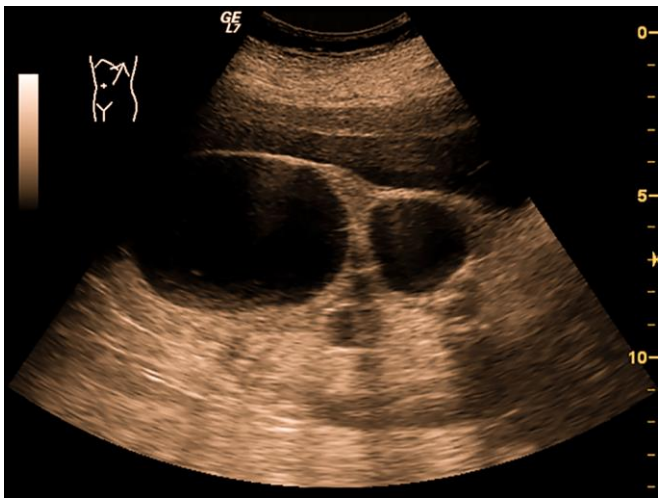

Focal changes of renal parenchyma

A change of architecture in an otherwise inconspicuous kidney parenchyma is called a focal modification. Cystic and solid forms of modification can be differentiated.

Cystic focal changes of the kidney parenchyma

Bosniak classicification

Bosniak group published in 1986 describing the differentiation of cystic lesions into 4 groups. It was based on imaging performed with contrast enhanced CT (CECT). Because many of Bosniak III lesions were benign and further group was added. Similar classifications of cystic lesions have been described using CEMR and contrast enhanced ultrasound (CEUS) [(39-41)].

1. Bosniak I: simple cyst (benign)
2. Bosniak II: minimally complex cyst (benign)
3. Bosniak IIF (follow): slightly more complex than II, not yet III (95% benign)
4. Bosniak III: complex cysts (40-60% malignant)
5. Bosniak IV: mixed cystic-solid lesion (85-100% malignant)

Bosniak classification criteria:

- septa
- cyst content
- contrasting
- solid shares

Bosniak I: Simple renal cyst

Wall	thin (< 1 mm)
septa:	no
cyst:	anechoic

contrast enhancing: no

solid components: no

A simple renal cyst forms approximately 65–70% of focal changes of the kidney. Its image consists of a smooth wall, posterior echo enhancement and tangential shadow [Figure 56]. The cysts usually grow with ageing. Up to 40% of adult patients have at least 1 simple kidney cyst.

Figure 56 Simple renal cyst (classified as Bosniak I).

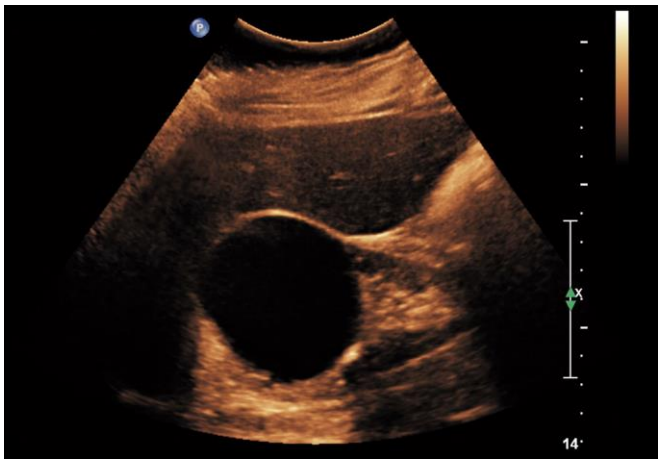

Calyx diverticulum

For the differential diagnosis, the sonographer has to differentiate between kidney cysts and calyx diverticulae. Calyx diverticulae usually narrow towards the kidney pelvis and some of them contain stones [Figure 57 and 58].

Figure 57 Calyx diverticulum.

Figure 58 Calyx diverticulum: contrast-enhanced ultrasound helps to differentiate from a cyst. The diverticulum has a clear connection to the collecting system.

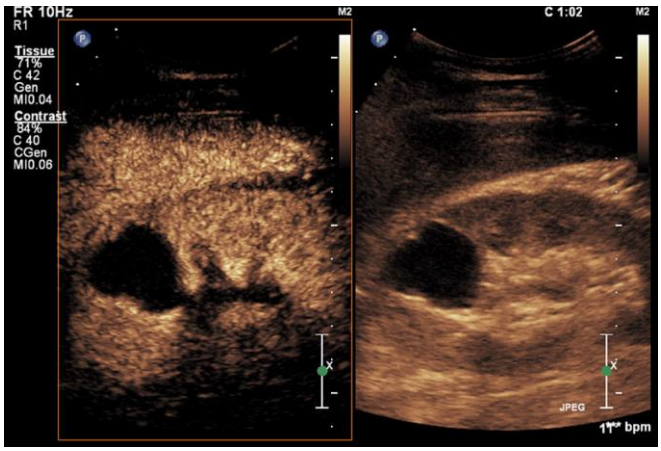

Lymphoma

Sometimes, cyst-like formations deveop due to non-Hodgkin's lymphomas [Figure 59]. CEUS proves helpful because compared to cysts, lymphomas are very well perfused.

Figure 59 Focal change in the kidney: cyst-like non-Hodgkin's lymphoma.

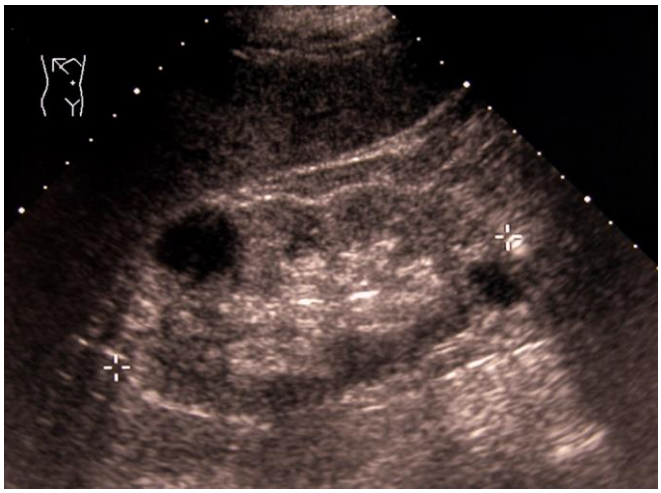

Bosniak II: complex renal cyst

wall	thin; partly slightly thickened/ calcified
septa:	few, see above
cyst:	anechoic or homogenous echogenic
contrast enhancing:	minimal
solid components:	no

Some cysts show thin septa and wall calcification. RCCs consist of cystic as well as solid parts. CEUS is helpful to differentiate cysts and mixed cystic-solid space [(42, 43).

Figure 60 Bosniak II: cyst with thin septa (a). Bosniak II: cyst with thin septa: in CEUS hardly perfused (b).

a

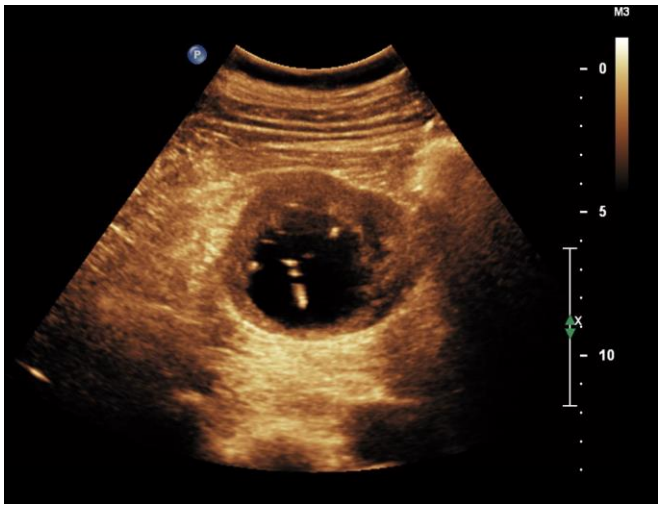

b

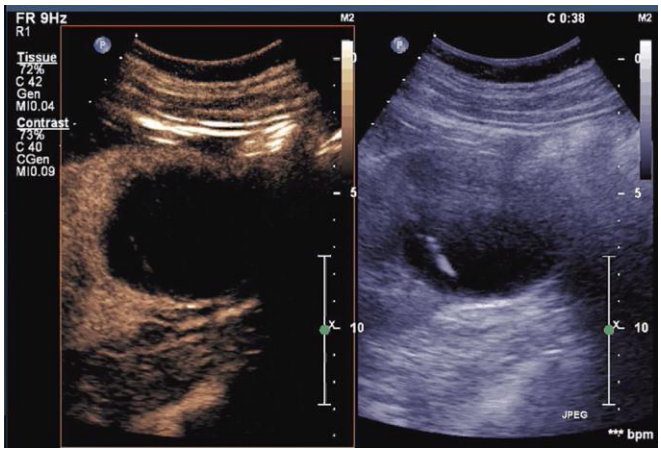

Bosniak IIf: complex renal cyst

wall	thin; partly slightly thickened/ calcified
septa:	many, see above; thickened, nodular
cyst:	anechoic or homogenous echogenic
contrast enhancing:	minimal
solid components:	no

Bosniak IIF (follow): homogenous echogenic cyst or, via CT, hyperdense cyst. Wall is thin, partly thickened or calcified. Criteria are many septa, slightly thickened or calcified, sometimes thickened or nodular. CEUS should be performed again after 6 months to avoid missing a malignancy [(44)]. An echogenic cyst that bleeds is represented on CEUS as a cyst

or non-perfused space [Figure 61a,b]. It can be clearly differentiated from a partly perfused space, which is likely to be a cyst holding a carcinoma. Perfusion of even the smallest solid part of a cyst should always be assumed to be a possible malignancy [Figure 62a,b].

Figure 61 Echogenic cyst on left kidney of patient (a). Contrast-enhanced ultrasound: cyst is not perfused. Simple renal cyst with bleeding (arrows), Bosniak II (b).

a

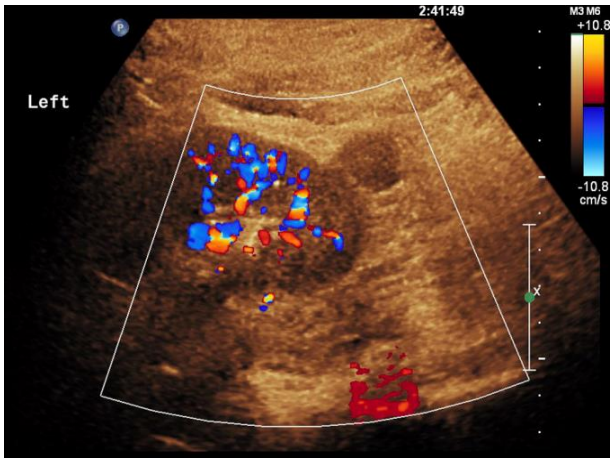

b

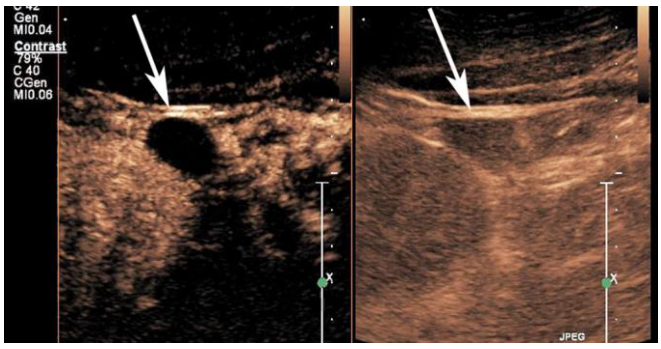

Figure 62 Echogenic cyst on right kidney of the same patient (a). Contrast-enhanced ultrasound in echogenic cyst: perfused solid part: Bosniak IV: Renal cell carcinoma (arrows) (b).

a

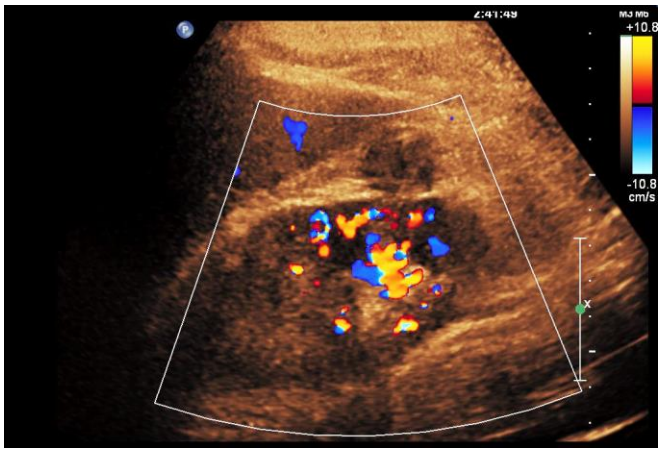

b

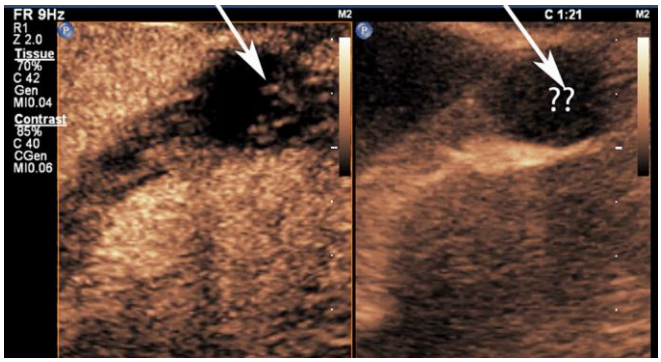

Bosniak III: complex renal cyst

wall	thin; partly irregular thickened/ calcified
septa:	many, see above; thickened, nodular
cyst:	anechoic or homogenous echogenic
contrast enhancing:	present
solid components:	no

Bosniak III: cysts with partly irregular and thickened, often calcified walls, many septa, thickened, nodular, with cyst content anechoic or homogenous echogenic [(45)]. Septa are perfused and this is better seen using CEUS compared to CECT. 40–60% of such changes prove to be malignant [Figure 63]. B-mode is not enough for assessing the changes in Bosniak III and IV. CEUS often brings surprises [Figure 64].

Figure 63 Cyst with thick septa (a). Cyst with thick septa, in CEUS strong perfused: Bosniak III (b).

a

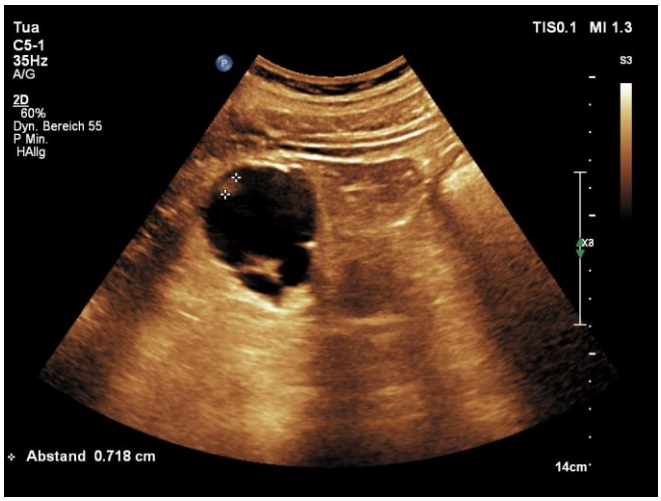

b

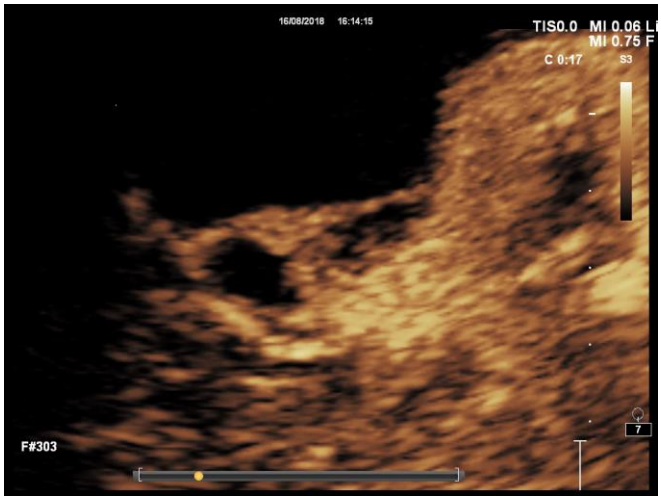

Figure 64 In CECT and CEMR suspicion of malignant tumour. Inhomogenous echoic formation in B-mode (a). Contrast-enhanced ultrasound: no perfusion, simple cysts with bleeding, Bosniak 2 (b). Contrast-enhanced ultrasound: TIC (Time intensity curve): no perfusion in bleeding cyst (blue) and cortex perfusion (red). (c).

a

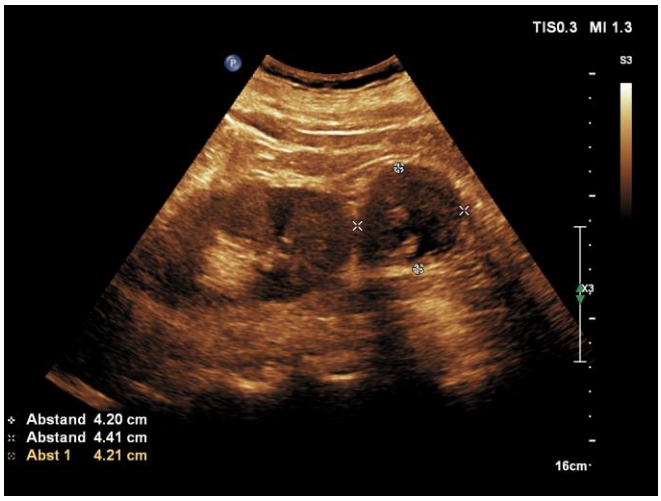

b

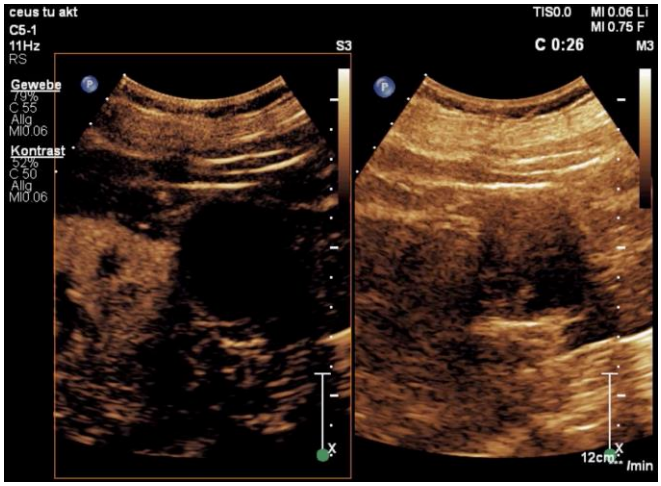

c

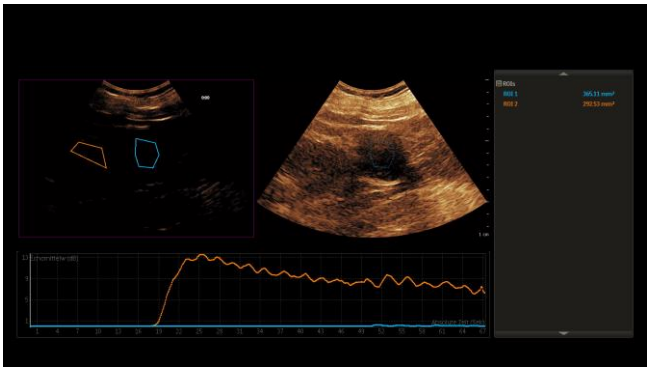

Bosniak IV: complex renal cyst

wall	thin; partly irregular thickened/ calcified
septa:	many, see above; thickened, nodular

cyst:	anechoic or homogenous echogenic
contrast enhancing:	present also solid shares
solid components:	present

Bosniak IV: cysts with solid parts, 85–100% are malignant. Usually, such cases are clear cell RCC with secondary regressive modifications and pseudocystic transformation[Figure 65a-b]. It can sometimes be a multilocular (cystic) clear cell RCC. It can be difficult to differentiate from a benign cystic nephroma [Figure 66] whose images can also show solid and cystic parts [(46, 47)].

Figure 65 Cyst with solid shares: debris (a)? cyst with solid shares: CEUS: perfusion of solid shares: = solid lesion, Bosniak IV. Result: clear cell renal cell carcinoma (b).

a

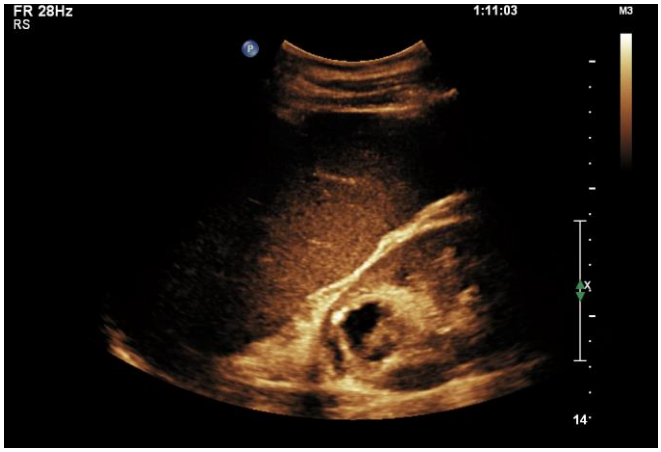

b

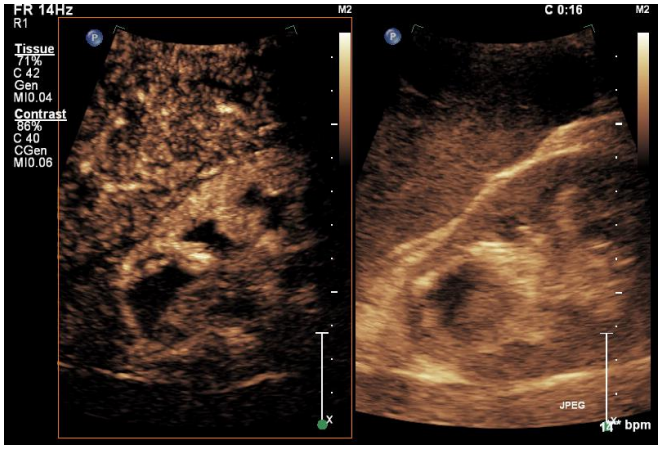

Figure 66 Benign cystic nephroma, difficult to differentiate to other Bosniak IV lesions (a) Benign cystic nephroma, difficult to differentiate to other Bosniak IV lesions: CEUS shows perfused septa and solid shares (b).

a

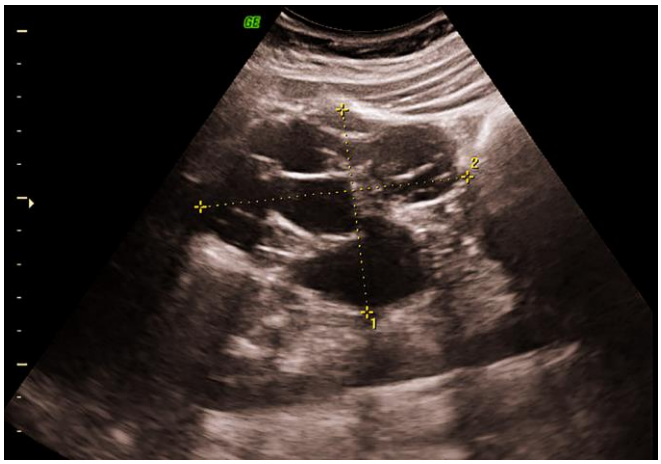

b

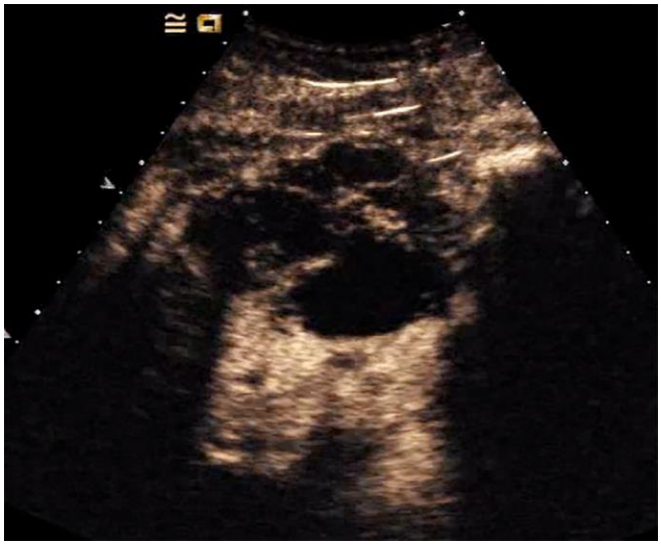

Solid focal changes of the kidney parenchyma

The differentiation of solid focal renal lesions is often not easy. First, it is important to distinguish the common benign changes, such as parenchymal cones, from true tumourous

changes. This is in most cases possible by careful presentation and analysis of B-mode images. Complementing with CDUS is useful in most cases. If, however, true tumours are suspected, measurement of tumour echo density [(48)] versus echogenic tumour cortex ratio (E-TCR), semiquantitative assessment of tumour vascular disease using CDUS, and assessment of CEUS behaviour including quantification of the tumour time intensity curves (TIC) is useful [(49-52)]. In addition to ultrasound we also have CECT and CEMR available. In special cases where the diagnosis remains uncertain an ultrasound-guided tumour biopsy should be performed.

Non-tumourous solid focal changes of the kidney parenchyma

These are to be differentiated from genuine tumours.

Renal parenchymal cone (RPC)

As a rule, this phenomenon results from an isoechoic formation leading into the renal sinus. It has been referred to as a hypertrophied column of Bertin [(53)]; however, a RPC is not always hypertrophy of the cortex. Some lobules reach deeper into the renal sinus [Figure 10,67,68]. Sometimes an entire lobule including the renal pyramid “falls” into the renal sinus [Figure 69]. As a result of the inhomogenity, these cases are doubtful and further investigation is recommended. RPC or pseudotumour is very common, in one study 53% of patients has at least one RPC [(54)]. Solid tumours are much less frequent: Angiomyolipoma 0.13-2.2% and renal cell carcinoma 0.11-0.9%. [(55-58)]. Because RPC is so frequent, clarifying with CT would bring enormous radiation exposure to the population [(59)] and therefore CEUS is the investigation of choice in unclear RPC cases [(60)].

Figure 67 Renal parenchymal tap with hypertrophied column of Bertin.

Figure 68 Renal parenchymal tap with hypertrophied column of Bertin.

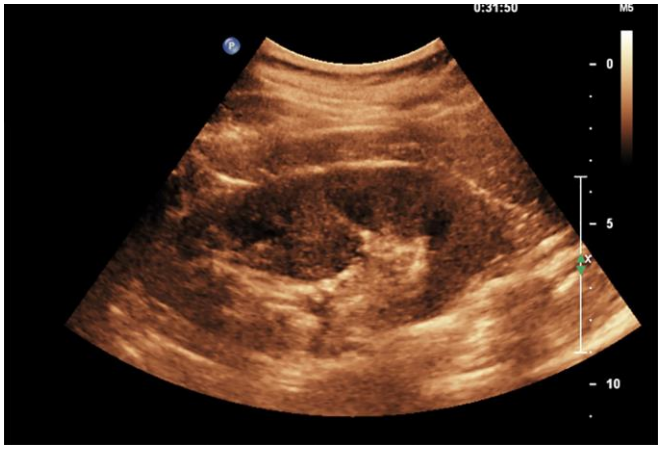

Figure 69 Renal parenchymal tap with the whole lobulus including the medulla in the renal sinus.

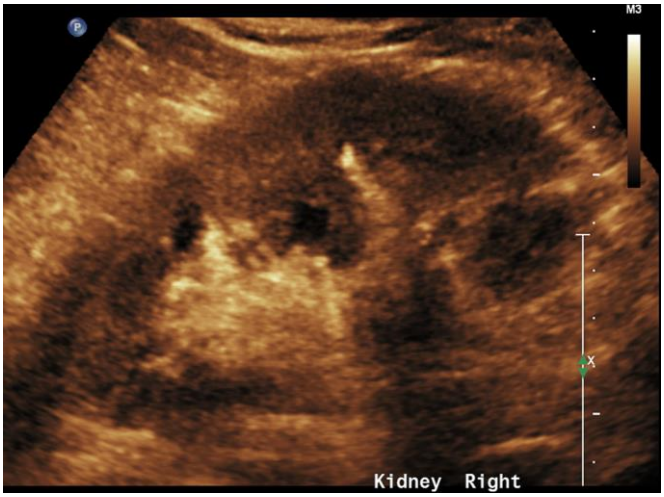

Lobar pyelonephritis

The infected lobule can be both hyper- and hypoechoic, is oedematous enlarged and, during PWDS or CDUS examination, perfusion is reduced [Figure 70,71]. This can lead to suspicion of a tumour and CEUS examination becomes crucial. In pyelonephritis hypoechoic areas are already visible on B-mode ultrasound and the possibility of a renal abscess should be taken into account. CEUS can reveal the start of an abscess because of its representation of non-perfused areas [(8)], which would remain undiscovered on B-mode ultrasound of an otherwise inconspicuous kidney parenchyma [Figure 72].

Figure 70 Hypoechoic lobar pyelonephritis with reduced CDUS-signals.

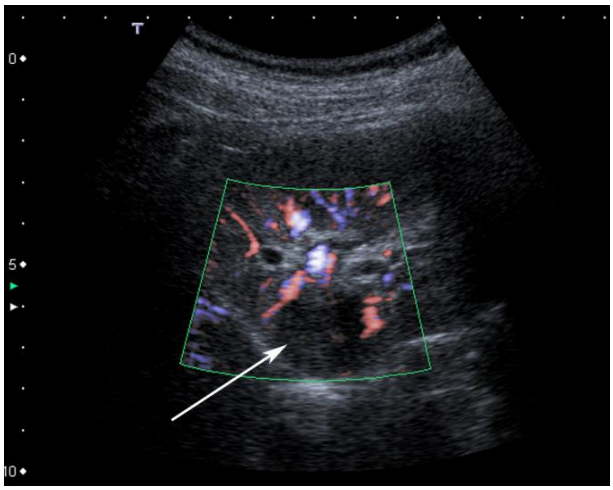

Figure 71 Hyperechoic lobar pyelonephritis with reduced CDUS-signals.

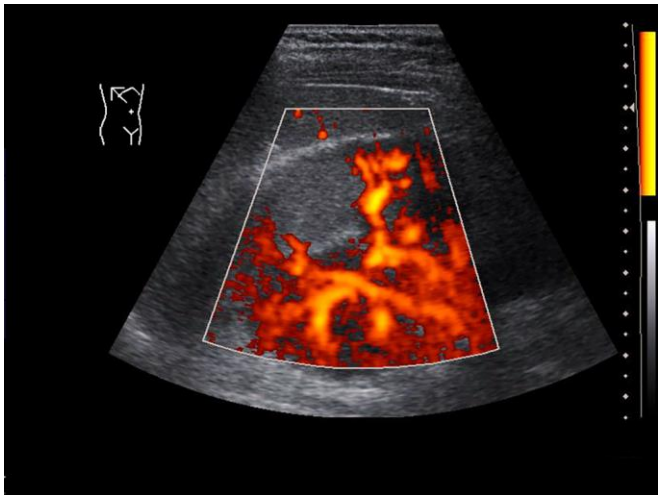

Figure 72 CEUS: No perfusion (left in picture) in the area of the abscess (arrow).

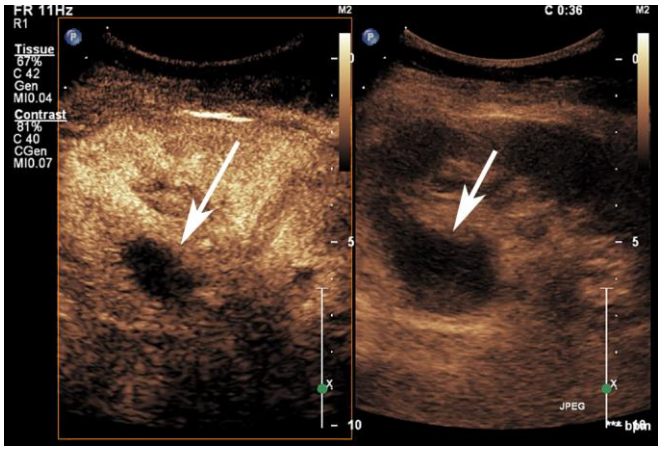

Medullary nephrocalcinosis

In some cases, medullary nephrocalcinosis can lead to a misdiagnosis of a multiple renal hyperechoic tumours [Figure 49].

Tumourous solid focal changes of the kidney parenchyma

Angiomyolipoma (AML)

This hyperechoic tumour consists of fat, vessels and fibrous tissue. It is seen relatively frequently with an occurrence of 0.11-2.2% [(55-57)]. As a rule, a strong hyperechoic structure of the tumour is of diagnostic importance [Figure 73,74]. Measurement of E-TCR is very useful [(48)]. Typical AML has E-CTR > 2.0 [Figure 75]. It is usually discovered accidentally. Tumours are often smaller than 1cm and show hardly any growth over the years. The small tumours are very well perfused and the inflow during CEUS [Figure 76] is almost as fast as that of the surrounding kidney cortex [(51)]. Larger tumours have slower influx. The assessment of larger angiomyolipomas can sometimes be difficult because larger tumours over 4 cm can bleed.

Figure 73 Hyperechoic angiomyolipoma.

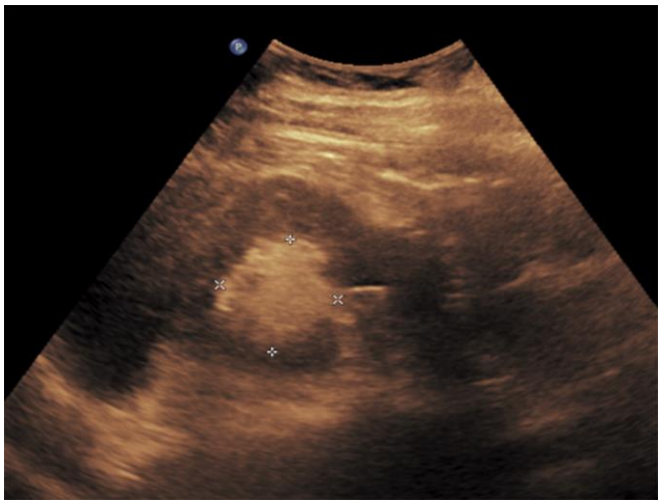

Figure 74 Hyperechoic angiomyolipoma.

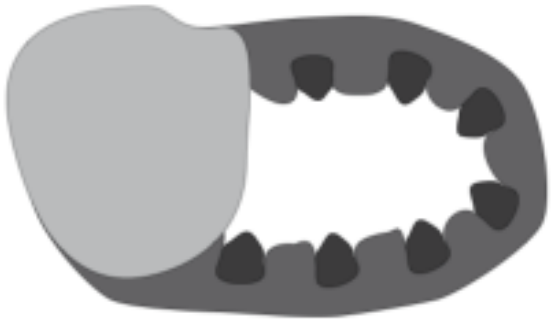

Figure 75 Hyperechoic angiomyolipoma: Measurent of E-TCR.

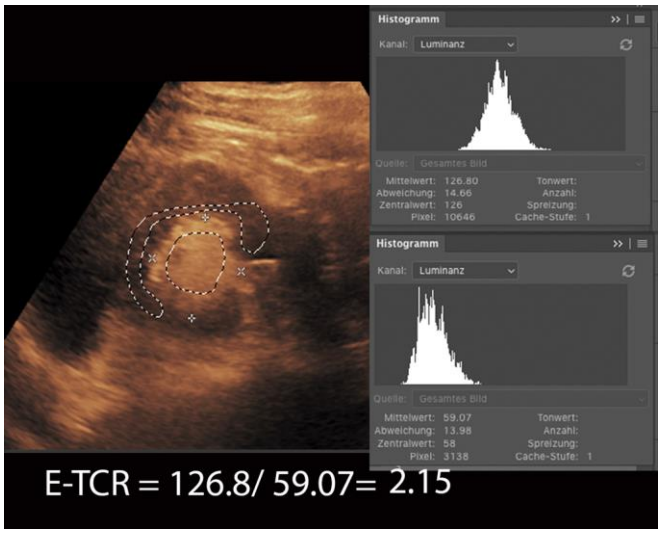

Figure 76 Hyperechoic angiomyolipoma: TIC of CEUS with as fast inflow of contrast in tumor (blue) as in cortex (red).

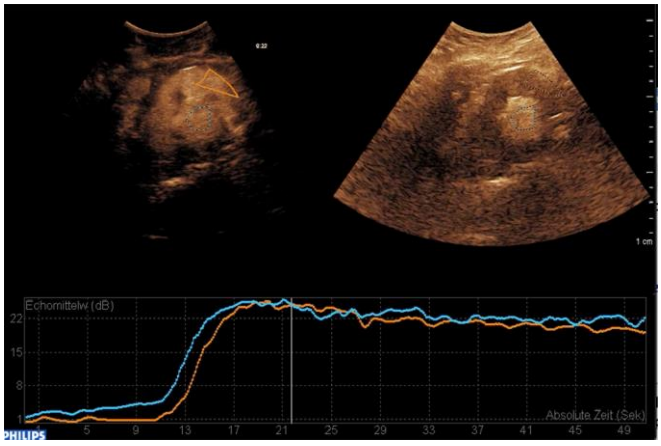

Hypoechoic and epitheloid variant of angiomyolipoma

Although angiomyolipomas are usually in the group showing hyperechoic focal changes, there is one variation of a tumour without any fat content. This is hypoechoic and is therefore not distinguishable from other hypoechoic masses. The epithelioid variant is very rare [(61)] often hypoechoic[Figure 77].

Figure 77 Two parts of AML: hyperechoic (classic, arrow 1) and hypoechoic (epitheloid variant, arrow 2).

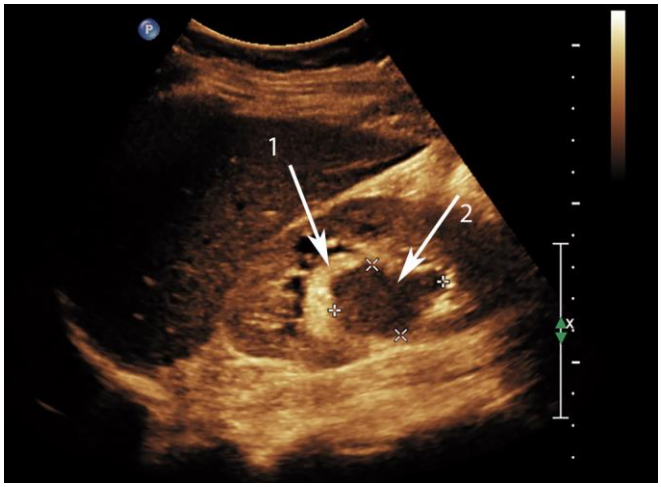

Renal cell carcinoma

The most significant malignant tumour in the kidney is RCC. It makes up approximately 3% of all malignancies. Of primary kidney tumours, approximately 90% are formed by RCC with the remaining are made up of embryonic carcinomas, nephroblastomas, sarcomas, neuroblastomas and other very rare tumours. RCCs are further classified and divided into clear cell carcinoma, papillary carcinoma, chromophobe carcinoma and collecting duct carcinoma. The differentiation of benign and malignant kidney tumours is often unsatisfactory on CEUS, CEMR and CECT, therefore increasing numbers of these tumours are biopsied under ultrasound guidance [(23, 62, 63)].

Clear cell renal cell carcinoma

This group is often hypoechoic or isoechoic, often inhomogenous [Figure 78–79a,b]. The E-TCR is almost below 2.0. These tumours are well perfused, which can be shown using CDUS, CEUS and CEMR. On CDUS there are often more than 3 tumour vessels visible [Figure 80]. On CEUS, these tumours are often faster and more strongly perfused than the renal cortex [Figure 81-82]. Perfusion of margins is increased in larger tumours, within the tumour's

necrotic areas with no or few perfusion. Outflow from the tumour is sometimes faster, sometimes almost the same as from the kidney cortex.

Figure 78 Clear cell renal cell carcinoma (CC RCC).

Figure 79 Clear cell RCC with central hypoechoic zone. R-TCR is below 2.0: 1.16 (a) Surgical specimen of the same tumour (b).

a

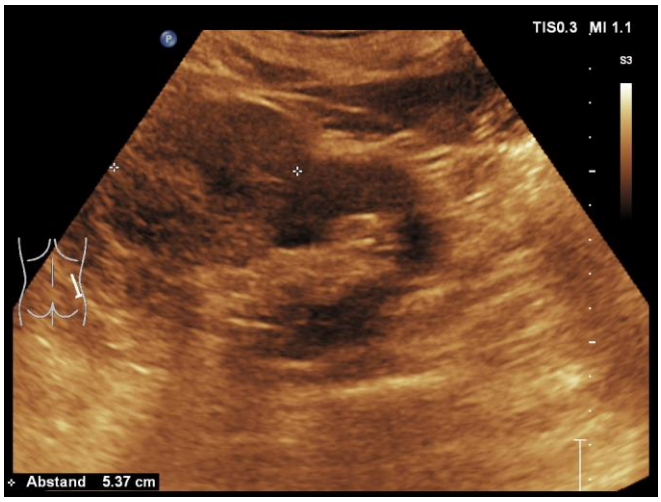

b

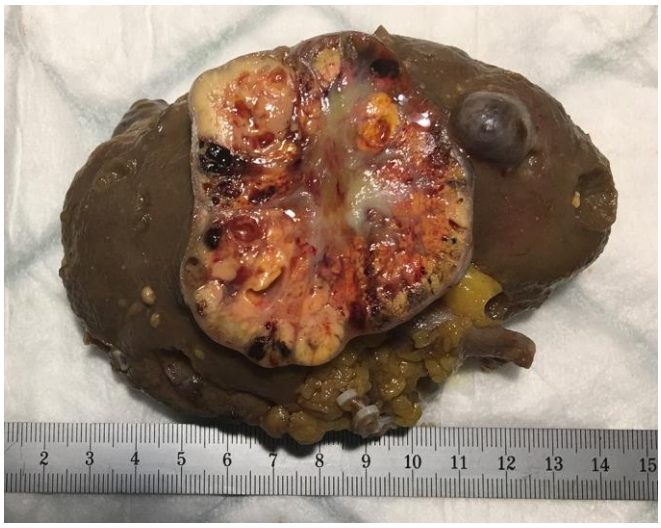

Figure 80 CDUS in CC RCC. More than 3 vessels visible in tumour.

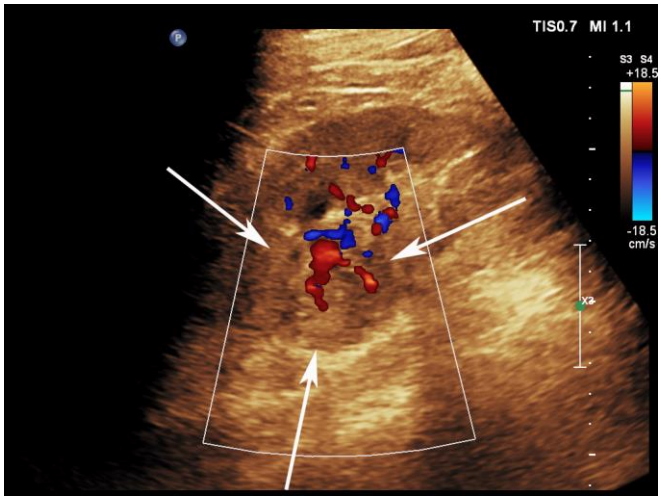

Figure 81 CEUS in CC RCC. Inflow is faster and more intense.

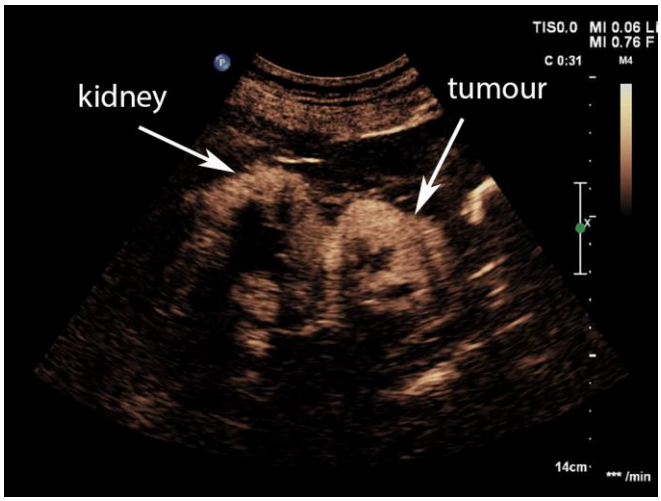

Figure 82 CEUS in CC RCC. TIC showing faster and more intense inflow of tumour (red) than renal cortex (blue).

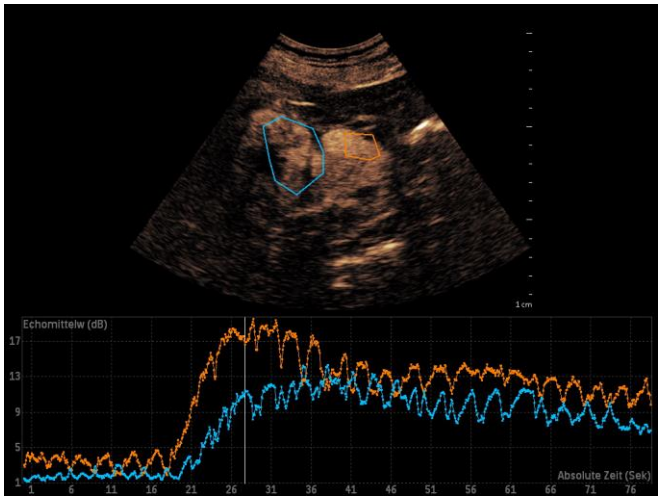

Papillary renal cell carcinoma

This is tumour, which is more homogenous, sometimes hypoechoic. [Figure 83]. E-TCR is below 2.0. CDUS shows less than 3, often no vessels in tumour [Figure 84]. In CEUS inflow is slower and weaker compared to renal cortex [Figure 85] and outflow faster than renal cortex [(49)].

Figure 83 More homogenous papillary RCC, E-TCR below 2.0: 1.53.

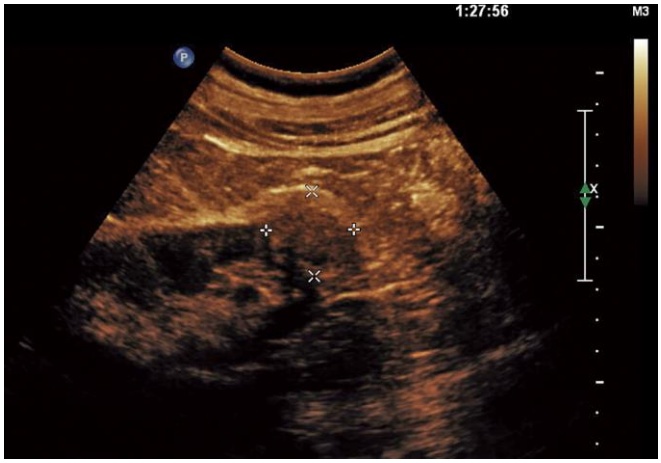

Figure 84 Power Doppler shows only 2 marginal vessels, none in tumour.

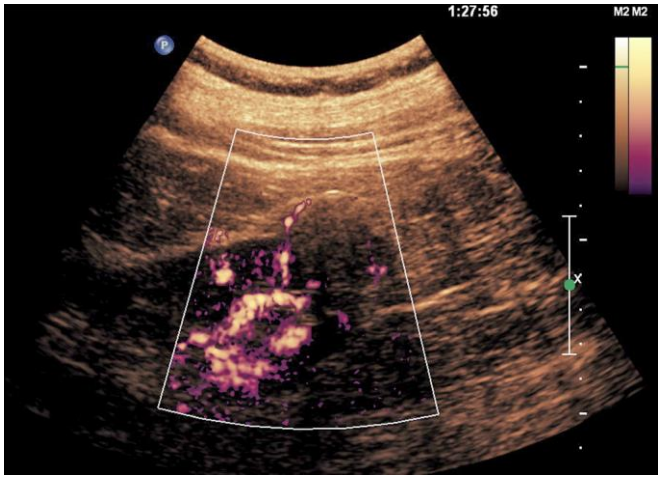

Figure 85 CEUS: TIC shows weaker perfusion of tumour (red), compared to renal cortex yellow).

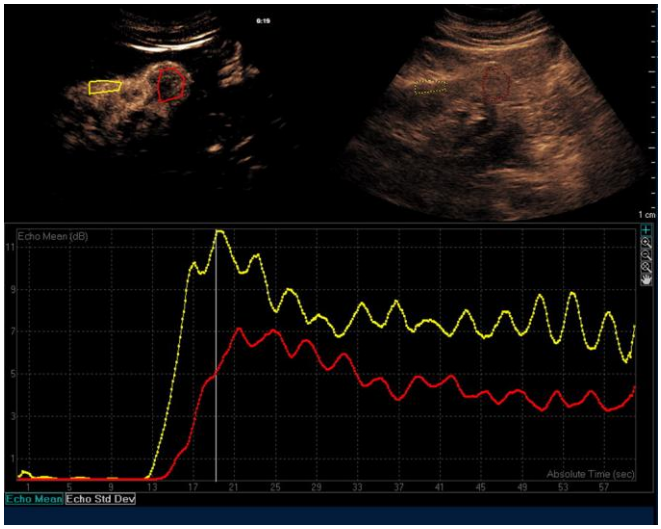

Oncocytoma

Oncocytoma is a benign tumour that is more echoic than the kidney cortex and is mostly homogeneous in structure. Scars located in the centre are quite a common finding [Figure 86 and 87]. On CEUS, a slow inflow from periphery to centre is visible [Figure 88 and 89]. TIC shows weaker inflow perfusion as CC RCC and faster outflow than renal cortex [Figure 90]. The tumour is usually indistinguishable from chromophobic carcinoma and, although this tumour is benign, it is often surgically removed.

Figure 86 Oncocytoma.

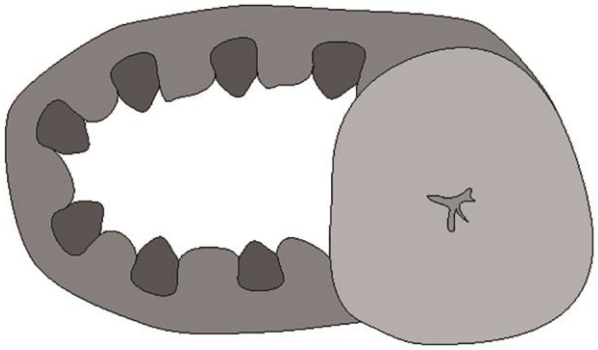

Figure 87 Oncocytoma on B-mode ultrasound. Homogenous tumour, E-TCR below 2: 1.52.

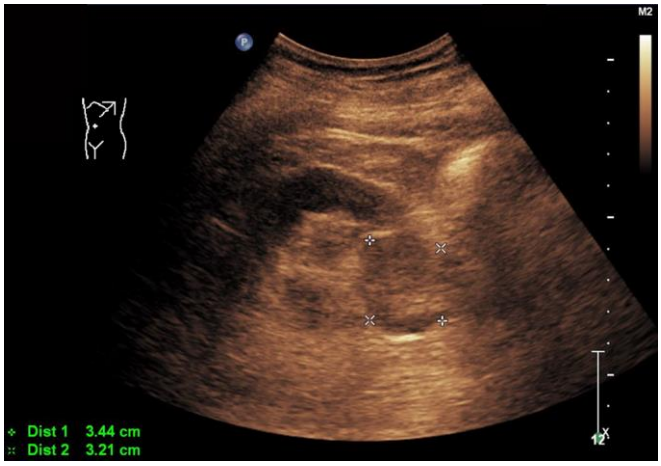

Figure 88 Contrast-enhanced ultrasound: oncocytoma with perfusion from periphery to the centre.

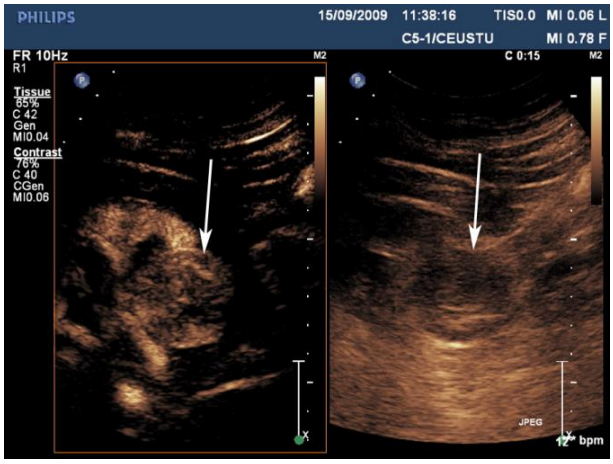

Figure 89 Surgical specimen of the same tumour as Figures 87-88.

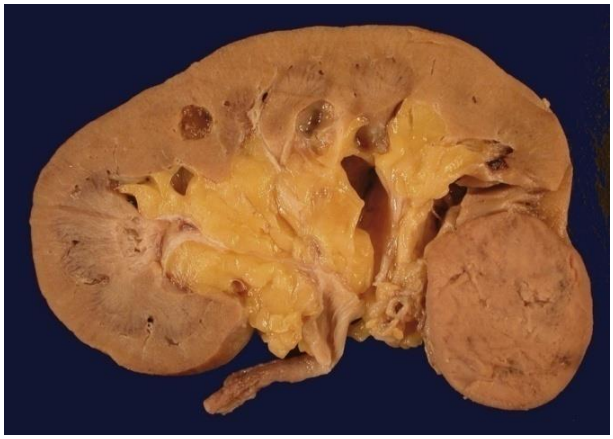

Figure 90 TIC of Oncocytoma: Tumour weaker and later (red) as renal cortex (yellow).

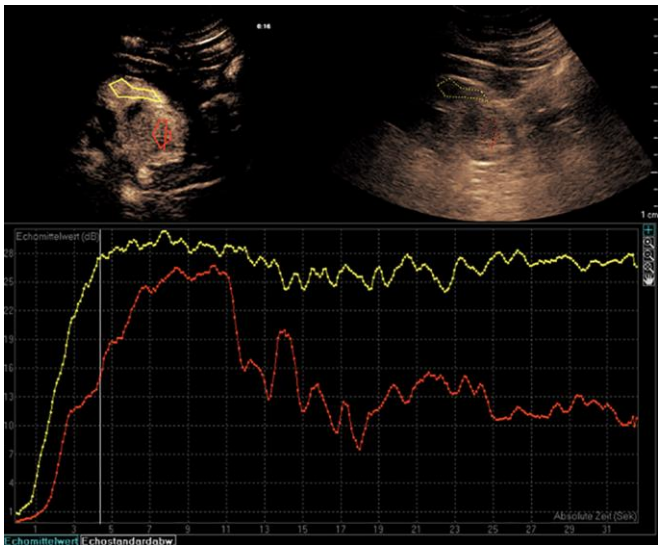

Chromophobic renal cell carcinoma

The sonographic characteristics of chromophobic RCC are like the ones of an oncocytoma. TIC of chromophobic RCC is very similar to oncocytoma [Figure 91]. Even histological differentiation of these tumours can be difficult.

Figure 91 Chromophobic RCC: TIC is very similar to oncocytoma: Tumour weaker and later (blue) as renal cortex (red).

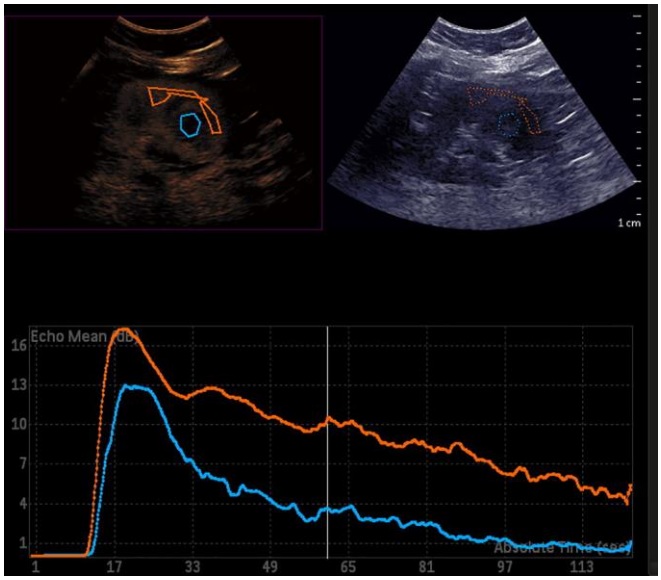

Renal cell adenoma

This mass is usually hypoechoic and occurs mostly in the cortex. In most cases it is a homogeneous tumour without necrotic areas, which is not distinguishable from small RCC.

Renal metastases

Metastases have been found in many tumours including lung cancer, ovarian cancer, leiomyosarcoma and neuroendocrine tumours. Since the introduction of CEUS, the detection rates have increased compared with those previously found on pathological-anatomical studies.

Bellini duct carcinoma (also known as collecting duct carcinoma)

Bellini duct carcinoma is very rare. It is slightly more echoic than the kidney cortex and is not distinguishable from other forms of carcinoma by B-mode ultrasound.

Complex focal changes of the kidney parenchyma

It can be difficult to differentiate between multicystic dysplastic kidneys and tumours, such as clear cell RCC or multilocular cystic RCC, because both can show solid and cystic or pseudocystic parts. In carcinomas there is always a part of the kidney intact, however small it might be, in contrast to multicystic dysplastic kidneys. Another change to the complex structure occurs in benign cystic nephroma, which is a benign tumour consisting of both cystic and solid parts and calcification [Figure 66, 92]. Although Wilm's tumour is usually structurally solidly with few cystic parts, variations of this tumour are found with almost only cystic parts. Even large angiomyolipomas can show significant bleeding and consist of a complex structure with areas that are hypoechoic.

Generally, tumours with a partly cystic and partly solid complex structure tend to be large. The diagnosis is problematic and even combined imaging (CEUS, CECT and CEMR) does not always lead to a definitive diagnosis. As a result, most cases, benign or not, are operated on.

Figure 92 Benign cystic nephroma.

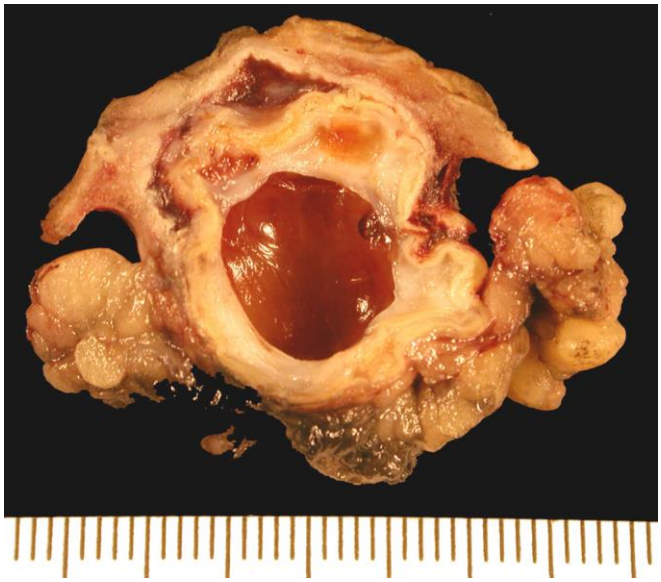

Changes of the kidney vessels

Changes in renal arteries

The kidney is well perfused. Approximately 1500 litres (l) of blood passes through daily, which leads to a production of approximately 150 l of primary urine and approximately 1–2 l of excreted urine per day. The crucial function of the kidney is to rinse the blood, *i.e.* glomerular ultrafiltration. Glomerular filtration rate (GFR), or rather the production of primary urine by ultrafiltration, serves as an important parameter for the analysis of kidney function. Normally, this value is approximately 150l per day or more than 90ml/min/1.73m^2 BSA, hence the very high perfusion rate. At rest, the kidney receives 20% of the cardiac output and 100g of kidney tissue has perfusion rate of 400ml/min. Like cerebral vessels, renal arteries have very low resistance. CDUS can depict renal arteries in both longitudinal and profile sections. The spectral curves of renal arteries are monophasic and as a result the evaluation of maximum systolic velocity (V_{max}) and minimum end-diastolic velocity (V_{min}) is possible and the RI (V_{max} - V_{min}/ V_{max}) can be calculated. Only 60% of all patients' kidneys

have one main artery, the rest have one or two polar arteries. On average, renal arteries have a diameter of 3.5–6.8mm. Accessory arteries have a smaller diameter of approximately 3–5mm. This reduced diameter can be helpful in identifying accessory arteries [(64)]. In the case of a diameter less than 4.1mm it is likely to be an accessory artery (with sensitivity and specificity of 95%); with a diameter of greater than 5.5mm is unlikely to be an accessory artery. The normal Doppler values are as followed: V_{max}, 70–180cm/s, V_{min}, 25–65cm/s, RI, 0.60–0.80. Colour duplex sonography is recommended for a diagnosis of renal artery stenosis and use of data derived from spectral curves by measurement systolic and diastolic velocities. Systolic velocity in the aorta is of further help by using the data and outcome of the reno-aortal ratio (RAR).

Renal artery stenosis

With haemodynamically significant stenosis (>50%), the following values [(65)] apply as relevant limits: V_{max}>200cm/s (sensitivity 92%, specificity 81%), RAR>2.5 (sensitivity, 92%; specificity, 79%) and the quotient between renal artery and interlobar artery [(66)] reno-interlobar ratio (RIR) >5 as well as the V_{max} of interlobar artery <15cm/s (sensitivity, 91%; specificity, 87%). A relevant stenosis may be treated with catheter dilatation. At high RI baseline (RI>0.80) it is however, unlikely [(10, 11)] to be successful [Figure 93]. There is debate as to whether revascularization therapy is better than medical therapy of hypertension [(67)].

Figure 93 Renal artery stenosis at the vessel origin in longitudinal section. V_{max} 2.84 m/s.

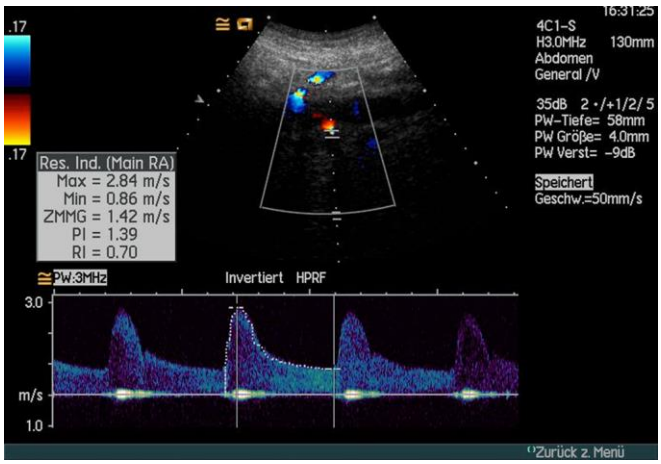

Arteriovenous fistula and aneurysms

Besides detecting renal artery stenosis and accessory renal arteries, evidence of arteriovenous fistula (after renal biopsy), aneurysmal broadened arteriovenous fistulas and aneurysms of renal arteries are important. The latter primarily consists of cystic changes, but can show pulsating changes on B-mode ultrasound, which should be clarified by CDUS.

Changes in renal veins

With adolescents or very slim patients, renal veins appear as anechoic and broad tubular structures, which can sometimes look like a broadened kidney pelvis [Figure 97]. CDUS can clarify this.

Nutcracker-phenomenon

The left renal vein runs over the aorta towards the vena cava. Sometimes it is compressed by the outgoing superior mesenteric artery, known as nutcracker-phenomenon. This is followed by stasis of the left kidney and orthostatic proteinuria and can, in extreme cases, lead to renal vein thrombosis [Figure 94].

Figure 94 Nutcracker-phenomenon with dilated left renal vein.

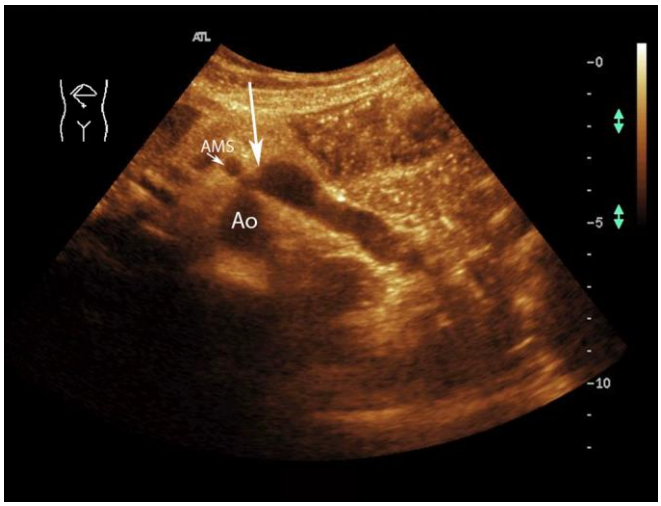

Renal vein thrombosis

In newborns, dehydration can lead to renal vein thrombosis. In cases of renal vein thrombosis on both sides, irreversible renal failure can occur. Owing to a loss of antithrombotic proteins, nephrotic syndrome can lead to secondary renal vein thrombosis; 65% of all patients suffering from renal vein thrombosis also show nephrotic syndrome. Thrombi in the renal veins are also found in malignant kidney disease. Differentiation between tumour thrombus and a blood clot can be easily distinguished on CEUS: a tumour is perfused and a clot is not [(23, 45)].

Changes after renal trauma

Perirenal, intrarenal and renal pelvis haematoma have all been observed. The rapid detection of traumatic kidney rupture is crucial [Figure 95]. If the situation is still ambiguous on B-mode ultrasound and CDUS, either CT or CEUS should be performed which will allow the rather indistinct changes of the kidney rupture to be detected. In blunt abdominal trauma, it is important to assess both the parenchymatous organs and the free liquid in the abdominal region. Besides kidney rupture, rupture of spleen and pancreatic contusion are quite common. In account of the high exposure of radiation from CT (full investigation with contrast is the equivalent of approximately 400 chest radiographs), CEUS is the preferred option, particularly in children and adolescents.

Figure 95 Kidney rupture on contrast-enhanced ultrasound.

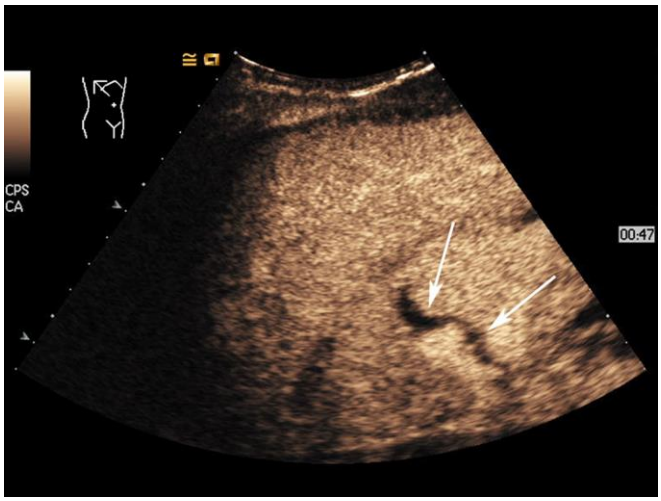

Upper urinary tract

Indications, examination technique and normal results

The examination of the upper urinary tracts consists of an assessment of the renal sinus and ureter as it progresses from the renal pelvis to bladder. This area is superimposed ventrally by the intestines and on ultrasound is therefore often covered by gas. Prone or a side position can help the examination. The first few centimetres, especially, are seen more clearly in a prone position and the outlet of the ureter is usually visible in this position. In most cases of only slightly broadened ureters a longer section, up to the iliac, can be shown. Examination is carried out either in a corresponding clinic, *i.e.* for cases of renal colic, when there is suspicion of urinary obstruction, or, incidentally and evidence of a change in the renal sinus is seen. It is important to examine the renal pelvis during the assessment of urinary tract infections. After the first section, between renal pelvis and iliac vessels examined in a prone position, further examination up to where the pelvic vessels cross, can be carried out in a side position or with the patient lying on their back. The last section of the ureter is often difficult to see. The best outcome is a representation of the ureteral orifice where the ureter can be traced back to the point where the pelvic vessels cross.

The normal findings of the renal sinus are hyperechoic structures, perirenal fat, renal vessels and the non-extended pelvis. In children and slim patients echo-free dilated renal veins are observed and this can lead them being confused with extensions of the collecting system. Also in children is the collecting system best assessed in a prone position and is usually clearly depicted; the ureter outlet is also clearly visible in this position [(68, 69)]. Only when the ureter is 2cm from the pyelo-ureteral transition and extended more than 5mm, is it referred to as a dilated.

Modifications of renal sinus

Anechoic renal sinus

Dilatation of the collecting system can occur during urinary obstruction, with vesicoureteral reflux or during pregnancy, where the collecting system appears anechoic. In cases of a slightly enlarged renal pelvis, it is particularly important to visualise the ureter.

Normal variations

On ultrasound the renal sinus can appear as either nearly inhomogeneous or completely homogeneous depending on the amount of sinus fat. In children and slim adolescents, who hold little sinus fat, anechoic tubular structures (mostly broad renal veins), part of collecting system and vessels can all be seen. In elderly people, the sinus fat can also appear highly hypoechoic, which can lead to confusion with dilatation of the collecting system (hydronephrosis).

Urinary obstruction

In cases of dilatation of the collecting system, anechoic spaces form, which intertwine with each other and dissociate from the remaining sinus. Depending on the level of obstruction, the following classification can be made:

- Intrarenal obstruction within tubuli and collecting ducts (*e.g.* acute gouty kidney).
- Calyceal obstruction (*e.g.* calyceal stenosis in tuberculosis).
- Obstruction at the pyelo-ureteral transition (*e.g.* with congenital stenosis).
- Ureteral obstruction (*e.g.* during passage of stones, necrotic papillae or blood clots).
- Infravesical obstruction (*e.g.* prostatic hyperplasia or urethral stenosis).

Furthermore, the distinction can be main between acute (hours to days), subacute (days to weeks) and chronic obstruction (months to years). An obstruction can occur either totally or partially; a total obstruction poses an urgent risk for the kidney. Obstruction located at the pyeloureteral transition, or distal from it, lead to a dilatation or congestion of the collection

system. Sonographic classification of the congestion is made with the help of changes in renal sinus, parenchymal thickness and spectral curve of interlobar artery.

Acute congestion

The volume of the affected kidney increases with acute congestion. There is an increase in density of echo in the kidney cortex [Figure 37] and a significant increase in the RI (change of ≥0.10 compared with the other kidney).

Chronic congestion

Chronic congestion leads to a gradual dilatation of the collecting system without any change in the RI values. The following stages of congestion can be made [Figure 96].

Figure 96 Stages of congestion: (a) normal, (b) degree I, (c) degree II, (d) degree III, (e) degree IV, (f) end-stage (irreversible hydronephrosis).

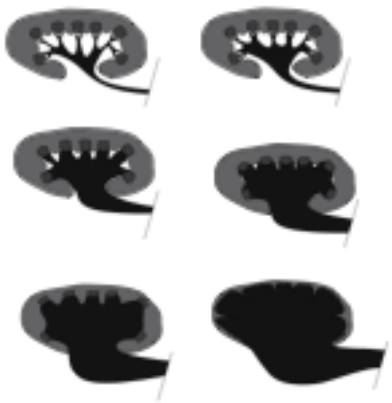

Stage I

Slight expansion of renal pelvis, while both renal pelvis and calices appear anechoic. 2cm from the pyeloureteral transition, the outgoing ureter should be at least 5mm wide.

Differential diagnosis for congestion Stage I

Stage I hydronephrosis can be simulated by widened renal veins. These tubular structures resemble the image of expanded collecting system [Figure 97]. However, renal veins do not leave caudally, but directly towards the large abdominal vessels. The use of CDUS is helpful in this situation.

Another form of variation of the renal pelvis is the ampullary renal pelvis, which is slightly prominent. Calyceal necks and ureters do not appear expanded and this can therefore be clearly distinguished from stage I congestion [Figure 98].

Figure 97 Prominent renal veins.

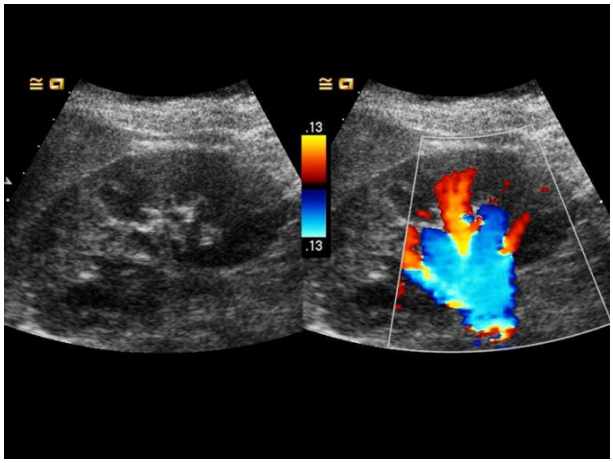

Figure 98 Ampullary renal pelvis.

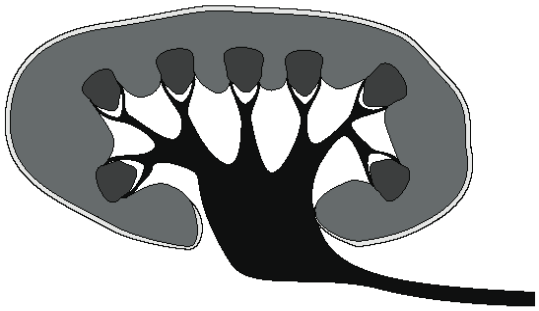

Stage II

Obvious expansion of pelvis, calyces and including calyceal necks. The fornix angle can still lie below 90° and the kidney parenchyma shows normal thickness.

Stage III

Pelvis and calyces, including calyceal necks, show obvious expansion and practically fill the whole renal sinus. Parts of the pelvis often already lie extra-renally. The parenchyma does not show any narrowing and the fornix angle lies above 90º [Figure 99].

Stage IV

There is significant narrowing of the parenchyma with a fornix angle usually above 120º. Further deterioration is the final stage where there is no recognisable parenchyma [Figure 100].

Figure 99 Congestion Stage III.

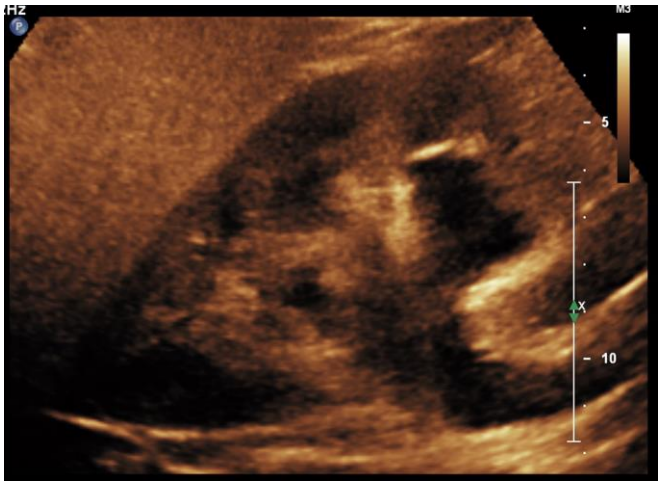

Figure 100 Congestion Stage IV: no visible parenchyma, “hydronephosis” with irreversible loss of kidney function

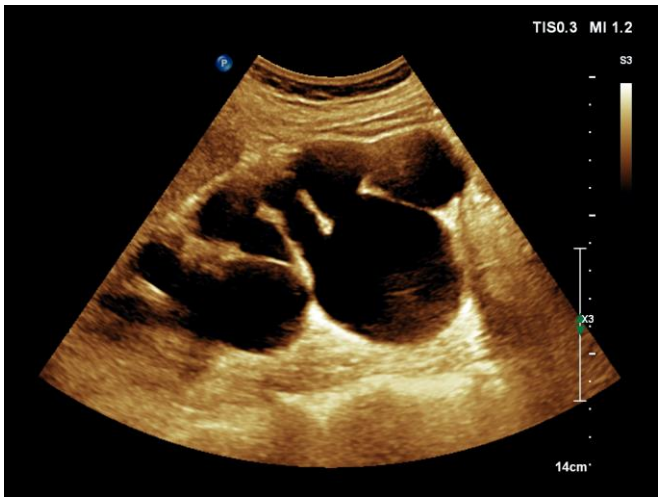

Differential diagnosis *for congestion Stage III-IV*

Megapolycalicosis

Megapolycalicosis is characterised by multiple calyces. This malformation originates from extremely short renal pyramids that are not visible in such images. Both the absence of renal

pyramids and the many and enlarged calyces are highly specific for this diagnosis [Figure 101]. There is no expansion of either the renal pelvis or the outgoing ureter.

Figure 101 Megapolycalicosis.

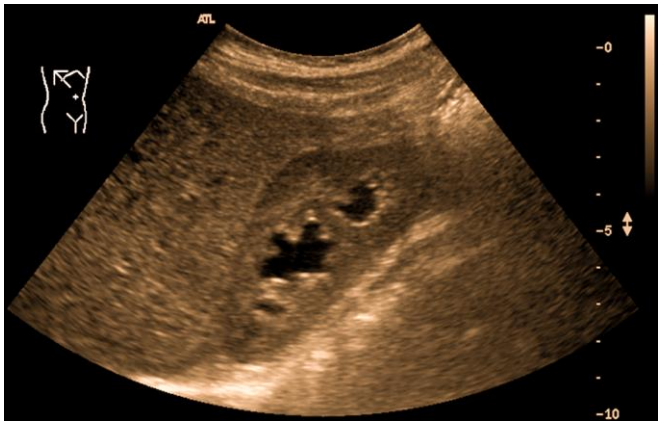

Parapelvic cysts

Another differential diagnosis simulating high-grade congestion is due to parapelvic cysts. With careful analysis of the image, the following criteria lead to a correct diagnosis: absence of calyectasia with a missing connection of single cysts to a renal pelvis and absence of an expanded ureter [Figure 102a-b].

Figure 102 Parapelvic cysts (a). Parapelvic cysts: no connection to pelvis (b).

a

b

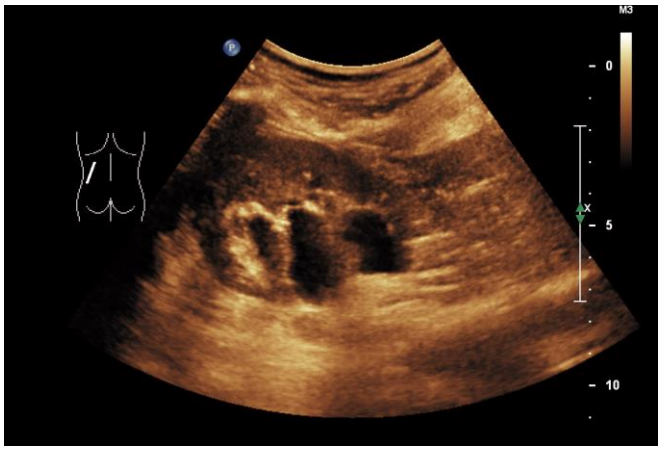

Hypoechoic renal sinus

Contrary to the fairly frequent finding of congestion, hypoechoic changes of the renal sinus rarely occur.

Haematoma

Haematoma, either post-traumatic or as a complication after renal biopsy or lithotripsy, are observed in the collecting system.

Transitional cell carcinoma (TCC)

Some tumours are located in the renal sinus. By far the most frequent is transitional cell carcinoma (TCC). It can be observed as a hypoechoic formation in the renal sinus [Figure 103]. Occasionally, diagnosis is only possible after additional examinations, such as CEUS, CECT or CEMR [(70)].

Figure 103 TCC: mostly hypoechoic (a). TCC: CEUS shows late weak perfusion only (b).

a

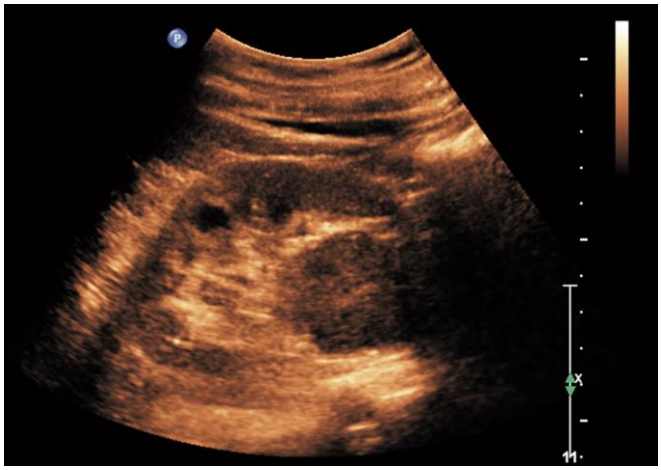

b

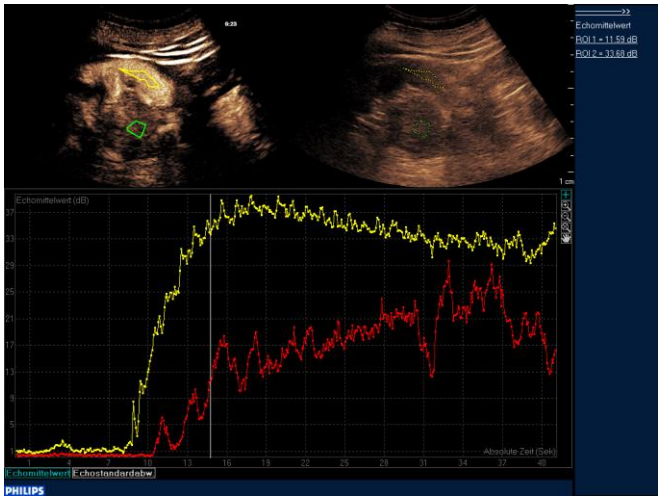

Hyperechoic renal sinus

Kidney stones

Above 5 mm size these strongly hyperechoic formations can be depicted on B-mode ultrasound. However, it is much more convenient to use CDUS to look for them. During examination, PRF should be set high and gain setting just below the artefact limit. With these settings, a colour artefact arises (so-called twinkling), which reveals hard reflectors in the area of the sinus [Figure 104a-b]. These artefacts occur in more than 80% of even the smallest, 1-2 mm kidney stones. The composition of the stones, calcium oxalate, calcium phosphate or uric acid, does not affect their ultrasound appearance, the twinkling artefact. Twinkling artefacts are not specific for any particular stone and are seen in calcification of vascular walls, of necrotic papillae in analgesic nephropathy, chronic pyelonephritis or occur during medullary nephrocalcinosis. Twinkling can also originate from intestinal gas.

Figure 104 Smaller stones are not easy to see in hyperechoic renal sinus (a). Stones are better visible with help of twinkling artifact (b).

a

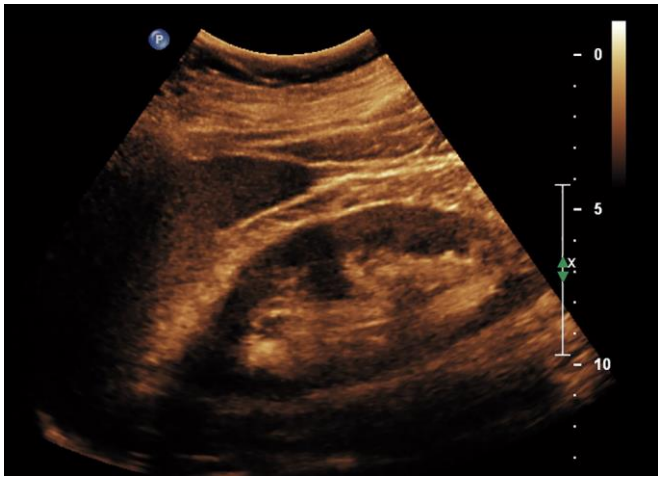

b

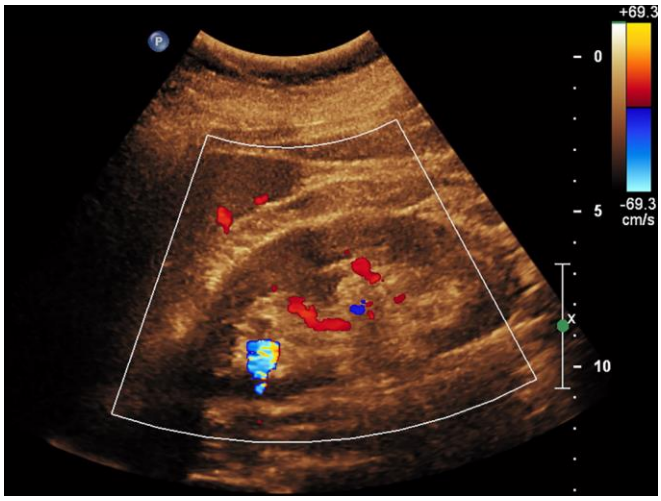

Changes of the ureter

Anechoic changes of the ureter

Hydro-ureter as a result of urinary obstruction

Renal colic

Kidney stones, blood clots and papillary necrosis passage are all causes of renal colic. They can provoke urinary obstruction and an expansion of the ureter, renal pelvis and calyces. In many cases, the cause for urinary obstruction can be shown on ultrasound. In typical renal colic, the presence of kidney stones [Figure 105] can be proved with a sensitivity of over 90% [(69, 71-74)] Looking for twinkling is very useful in this scenario because tiny stones in the ureter are very difficult to depict. It is convenient to start the examination in a prone position to scan the first few centimetres up to the iliac bone and then proceed to the prevesical spaces as well as the space at the point where the large vessels cross. Stones are often found owing to a twinkling artefact [Figure 105] and it is only afterwards that a typical hyperechoic reflex is seen; it sometimes shows a very fine acoustic shadow or none at all.

Figure 105 Hydroureter with stone and twinkling artefact.

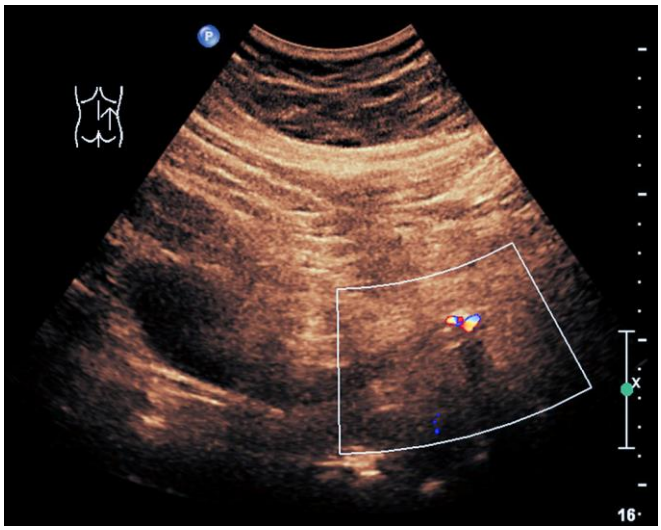

Differential diagnosis renal colic

If an acute renal arterial embolism is suspected, it is sensible to immediately proceed to CEUS. In case of a corresponding medical history (*e.g.* atrial fibrillation) evidence can be shown on CEUS and fibrinolytic therapy can be started immediately if infarctus from embolius is suspected [(6, 9, 45)(75)].

Painless (chronic) urinary obstruction with hydroureter

As well as acute renal colic there are other conditions, which show gradual narrowing of the ureter with both chronic inflammation of the ureter (e.g. ureteric tuberculosis) and ureteric tumours. Another cause of gradual expansion can be very large myomas, which cause external pressure on the ureter. Tumours lying retroperitoneal and retroperitoneal fibrosis can slowly lead to an obstruction of the ureter. As all these conditions proceed slowly, hydroureter is usually painless. In most cases it is discovered incidentally during systematic abdominal examinations.

Hydroureter with non-obstructive condition

Mega-ureter

This malformation of the ureter occurs with primarily dilated ureters.

Vesicoureteral reflux

This is a malformation of the vesicoureteral transition with a refluxing ureter. In cases of higher grade reflux, not only the terminal, but the whole of the ureter is dilated. The diagnosis of vesicoureteral reflux is particularly important in children with recurrent urinary tract infections. In addition to voiding cystourethogram (VCUG), which has the disadvantage of radiation exposure, sonographic voiding cystourethogram (SVCUG) with echo-contrast agents is now possible. So far this method has only been carried out in a small number of clinics, but this should increase over the next few years. Both the sensitivity and specificity of this examination method is as precise as VCUG [(75)].

Hypoechoic ureter changes

An expanded ureter can be anechoic with serious purulent infections. This is called a pyoureter, in which ureter catheters in the ureter can be tracked as hypoechoic formations. TCC is also hypoechoic and forms an obstruction in the ureter [Figure 106].

Figure 106 TCC in ureter.

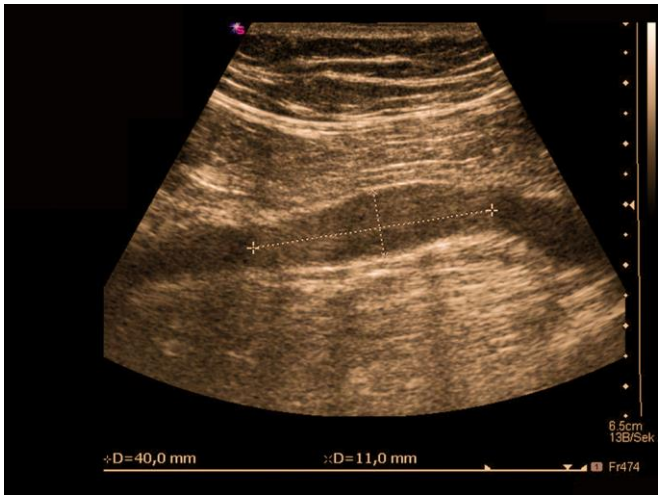

Hyperechoic ureter changes

Ureteric stones

The most important hyperechoic modification of the ureter is ureteric stones [Figure 105]. The procedure of following the outgoing ureter in a prone position, and in supine while crossing the pelvic vessels as well as following the ureter from ureteral orifice back to the crossing with the pelvic vessels has already been described. With dilated ureters, the search is carried out along the visible anechoic ureter. In unclear cases, CDUS is recommended with a high PRF setting and a gain setting just below the artefact limit to identify twinkling. Whether twinkling is seen or not is not dependent on the composition and roughness of the stones, but there is a correlation with the surface roughness. It has been shown during examinations that the same, freely floating stone in the bladder can show a very strong twinkling artefact once and then a very weak one or none at all depending on the position of the stone to the Doppler signal.

Twinkling is produced in more than 80% of ureteral stones [(72)], which is of diagnostic significance. However, twinkling artefacts are non-specific. Twinkling caused by intestinal gas has to be distinguished from stones and a history of papillary necrosis. Papillary necrosis has a triangular form and is only partially calcified, so distinction from stones can be made on B-mode ultrasound.

Urinary jet

The diagnosis of urinary tract obstructions can be quite demanding. Smaller kidney stones partly cause cases of discrete hydronephrosis and there is no difference in RI, so further diagnostic methods can be helpful. Urinary jet is a Doppler phenomenon showing inflow of urine into the bladder. With normal drinking habits of approximately 2–3 litres a day, an occurrence of 2 urinary jets/min or 10 urinary jets 5 minutes has been observed, on both sides. A jet asymmetry is defined by <2 jets/5min on the affected side and >5 jets/5min on the other side. As well as the number of jets, the quality of jets can also be assessed. A spectral analysis can provide results on both maximal velocity V_{max} and duration of the jets in seconds. With ureters that are not completely obstructed, jets appear to run slower and to last longer, while shorter jets are observed from time to time [(76, 77)].

Figure 107 Urinary jet: in Doppler two red urine streams coming from two ureters into bladder are visible.

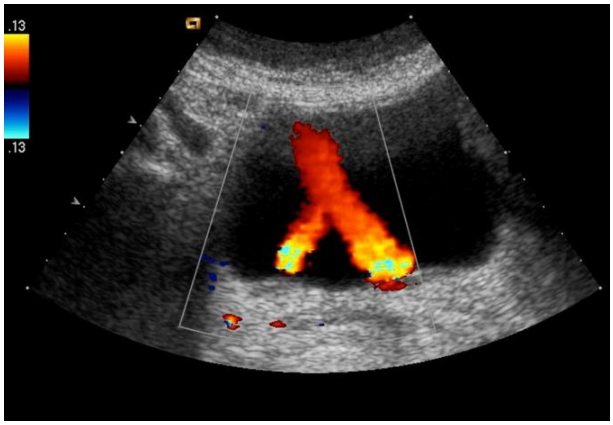

Ureteric colic diagnosis

As well as this very direct verification of a stone there are also some indirect signs of ureterolithiasis:

- non-glomerular haematuria;
- hydronephrosis, requiring minimal ureteral dilatation of 5mm, 2cm from the pyeloureteral transition;
- increase of RI ≥0.10 on the affected side;

A combination of two to three of these indirect signs indicates a very probable stone. In a prospective study, probable and directly verified stones by means of sonography amounted to 98% sensitivity for ureter stones [(69)]. As a further possibility, the asymmetry of urinary jets suggests one-sided obstructions of the urinary tract. An appropriate examination technique can help to reduce the number of stone clarifications carried out by the means of CT, which has the significant radiation exposure [(59)] In prospective study with 2382 patients sensitivity of US and CT was 85 resp. 86%, no statistical difference, it means, in renal colic do ultrasound first [(78)].

References

1. Emamian SA, Nielsen MB, Pedersen JF, Ytte L. Kidney dimensions at sonography: correlation with age, sex, and habitus in 665 adult volunteers. AJR Am J Roentgenol. 1993;160:83-86.

2. Tuma J, Trinkler F, Bock A, Dietrich C, Hollerweger A, Jenderka K. Sonographische Differentialdiagnose: Krankheiten des Urogenitalsystems. 1 ed. Köln: Deutscher Ärzte-Verlag, 2009.

3. Adibi A, Naini AE, Salehi H, M: M. Renal Cortical Thickness in Adults with Normal Renal Function Measured by Ultrasonography. Iran J Radiol 2008;5:163-166.

4. Beland MD, Walle NL, Machan JT, Cronan JJ. Renal cortical thickness measured at ultrasound: is it better than renal length as an indicator of renal function in chronic kidney disease? AJR Am.J Roentgenol. 2010;195:W146-W149.

5. Tuma J: Diffuse Nierenparenchymveränderungen: Niere mit Konturveränderungen. In: Tuma J, Trinkler, F, ed. Sonographische Differenzialdiagnose - Krankheiten des Urogenitalsystems Köln: Deutscher Aerzte Verlag, 2009; 77-81.

6. Bertolotto M, Martegani A, Aiani L, Zappetti R, Cernic S, Cova MA. Value of contrast-enhanced ultrasonography for detecting renal infarcts proven by contrast enhanced CT. A feasibility study. Eur.Radiol 2008;18:376-383.

7. Claudon M, Cosgrove D, Albrecht T, Bolondi L, Bosio M, Calliada F, Correas JM, et al. Guidelines and Good Clinical Practice Recommendations for Contrast Enhanced Ultrasound (CEUS) - Update 2008. Ultraschall in der Medizin 2008:28-44.

8. Granata A, Andrulli S, Fiorini F, Basile A, Logias F, Figuera M, Sicurezza E, et al. Diagnosis of acute pyelonephritis by contrast-enhanced ultrasonography in kidney transplant patients. Nephrol.Dial.Transplant. 2011;26:715-720.

9. Seeler D, KlinggrSff G, Christl SU. Sonographischer Nachweis des embolischen Niereninfarktes mit Echokontrastmittel. Ultraschall in der Medizin 2005:518-523.

10. Radermacher J, Chavan A, Bleck J, Vitzthum A, Stoess B, Gebel MJ, Galanski M, et al. Use of Doppler Ultrasonography to Predict the Outcome of Therapy for Renal-Artery Stenosis. The New England Journal of Medicine 2001;344:410-417.

11. Krumme B, Donauer J. Atherosclerotic renal artery stenosis and reconstruction. Kidney Int 2006;70:1543-1547.

12. Krumme B, Grotz W, Kirste G, Schollmeyer P, Rump LC. Determinants of intrarenal Doppler indices in stable renal allografts. J Am Soc Nephrol 1997;8:813-816.

13. Tuma J: Niere mit abnormer Form. In: Tuma J, Trinkler, F, ed. Sonograaohische Differentialdiagnose: Krankheiten des Urogenitalsystems. Köln: Deutscher Ärzteverlag, 2009; 69-75.

14. Tuma J: Diffuse Nierenparenchymveränderungen. In: Tuma J, Trinkler, F, ed. Sonographische Differenzialdiagnose - Krankheiten des Urogenitalsystems Köln: Deutscher Aerzte Verlag, 2009.

15. Rosenfield AT: Ultrasound evaluation of renal parenchymal disease and hydronephrosis. Urol.Radiol. 1982;4:125-133.

16. Hricak H, Cruz C, Romanski R, Uniewski MH, Levin NW, Madrazo BL, Sandler MA, et al.: Renal parenchymal disease: sonographic-histologic correlation. Radiology 1982;144:141-147.

17. Tuma J, Delmore G, Reutter F, Bürgin M: Die Nierenparenchymerkrankungen im Ultraschall. In: Ultraschalldiagnostik 83: Thieme Verlag Stuttgart, 1984; 140-142.

18. Tuma J, Schwarzenbach HR, Novakova B, Jungius KP, Kuchta M. [The quantitative measurement of the echogenicity of the renal parenchyma]. Praxis (Bern 1994) 2008;97:297-303.

19. Bohle A, Christ, H, Grund KE et al. The role of the interstitium of the renal cortex in renal disease. Contrib.Nephrol. 1979;16:109-114.

20. Moghazi S, Jones E, Schroepple J, Arya K, McClellan W, Hennigar RA, O'Neill WC. Correlation of renal histopathology with sonographic findings. Kidney Int 2005;67:1515-1520.

21. Rosner MH OM: Pathogenesis and etiology of ischemic acute tubular necrosis. In: S M, ed. UpToDate. MA: Waltham, 2017.

22. Feuchtner G, Frauscher F, Pallwein L, Schuster A, Klauser A, Helweg G, A. S. Die Pyelonwanddicke (PWD) als sonographisches Diagnosekriterium für akute Pyelonephritis. Ultraschall 2002;23:S72.

23. Wilson SR, Burns PN. Microbubble-enhanced US in body imaging: what role? Radiology 2010;257:24-39.

24. Bohle A WM, Eissele R et al. The long-term prognosis of AA and AL renal amyloidosis and the pathogenesis of chronic renal failure in renal amyloidosis. Pathol.Res.Pract. 1993;189:316-331.

25. Tuma J. [Kidney parenchyma diseases]. Praxis (Bern 1994) 2001;90:675-677.

26. Manley JA, O'Neill WC. How echogenic is echogenic? Quantitative acoustics of the renal cortex. Am.J Kidney Dis. 2001;37:706-711.

27. Korkes F, Favoretto RL, Br£glio M, Silva CA, Castro MG, Perez MDC. Xanthogranulomatous Pyelonephritis: Clinical Experience with 41 Cases. Urology 2008;71:178-180.

28. Slovis TL BJ, Gruskin A. Hyperechoic kidneys in the newborn and young infant. Pediatr.Nephrol 1993;7:294–302.

29. Kist-van Holthe JE vZP, Schell-Feith EA, Zonderland, HM HH, Wolterbeek R et al. Is nephrocalcinosis in preterm neonates harmful for long-term blood pressure and renal function?. Pediatrics 2007;119:468–475.

30. Tuma J, Jenny S: Echoreiche Markpyramiden: eine Folge des Furosemid-Abusus? Ultraschall in Klinik und Praxis 1990;5:233.

31. Kim YG KB, Kim MK, Chung SJ, Han HJ, Ryu JA et al.: Medullary nephrocalcinosis associated with long-term furosemide abuse in adults. Nephrol.Dial.Transplant. 2001;16:265–267.

32. Strauss S RG, Itzchak Y. Renal sonography in Bartter syndrome J Ultrasound Med 1987;6:265–267.

33. Zollinger HU: Chronic interstitial nephritis caused by the abuse of analgetics containing phenacetin (Saridon etc.) Schweiz.Med Wochenschr. 1955;85.

34. Mihatsch MJ ZH. Analgesic nephropathy. Zentralbl. Allg.Pathol. 1986;132:395–411.

35. P. K-S. Analgesic nephropathy. J Kidney Dis.Transpl. 1999;10:498–502.

36. Hateboer N DM, Bogdanova N, Coto E, Saggar-Malik AK, San Millan JL et al. Comparison of phenotypes of polycystic kidney disease types 1 and 2. European PKD1-PKD2 Study Group. Lancet 1999;353:103–107.

37. O'Neill WC RM, Bae KT, Grantham JJ, Chapman AB, Guay-Woodford LM et al. Sonographic Assessment of the Severity and Progression of Autosomal Dominant Polycystic Kidney Disease: The Consortium of Renal Imaging Studies in Polycystic Kidney Disease (CRISP). American Journal of Kidney Diseases 2005;46:1058–1064.

38. DH. T. Can.Assoc.Radiol.J 1986;37:161–163.

39. Bosniak MA. The current radiological approach to renal cysts. Radiology 1986;158:1-10

40. Israel GM, Bosniak MA. An update of the Bosniak renal cyst classification system. Urology 2005;66:484-488.

41. Park BK, Kim B, Kim SH, Ko K, Lee HM, Choi HY. Assessment of cystic renal masses based on Bosniak classification: comparison of CT and contrast-enhanced US. Eur J Radiol 2007;61:310-314.

42. Ignee A, Straub B, Schuessler G, Dietrich CF. Contrast enhanced ultrasound of renal masses. World J Radiol 2010;2:15-31.

43. Ignee A, Straub B, Brix D, Schuessler G, Ott M, Dietrich CF. The value of contrast enhanced ultrasound (CEUS) in the characterisation of patients with renal masses. Clin.Hemorheol.Microcirc. 2010;46:275-290.

44. Nilsson A. Contrast-enhanced ultrasound of the kidneys. Eur.Radiol. 2004;14 Suppl 8:104-109.

45. Sidhu PS, Cantisani V, Dietrich CF, Gilja OH, Saftoiu A, Bartels E, Bertolotto M, et al. The EFSUMB Guidelines and Recommendations for the Clinical Practice of Contrast-Enhanced Ultrasound (CEUS) in Non-Hepatic Applications: Update 2017 (Long Version). Ultraschall in Med 2018;39:e2-e44.

46. Carlson DH, Carlson D, Simon H: Benign multilocal cystic nephroma. American Journal of Roentgenology 1978;131:621-625.

47. Hsiao H L, Wu, W. J. Chang M Y, Ke H L, Huang C H.: Unusual Case of Multilocular Cystic Nephroma Treated with Nephron Sparing Technique: A Case Report Kaohsiung J Med Sci 2006;22:515-518.

48. Tuma J, Novakova B, Schwarzenbach HR, Jungius KP, Hollerweger A, Zatura F, Kuchta M, et al. [Image analysis in the differential diagnosis of renal parenchyma lesions]. Ultraschall Med 2011;32:286-292.

49. Xue LY, Lu Q, Huang BJ, Li CX, Yan LX, Wang WP. Differentiation of subtypes of renal cell carcinoma with contrast-enhanced ultrasonography. Clin Hemorheol Microcirc 2016;63:361-371.

50. Zhang J, Lefkowitz RA, Ishill NM, Wang L, Moskowitz CS, Russo P, Eisenberg H, et al.: Solid renal cortical tumors: differentiation with CT. Radiology 2007;244:494-504.

51. Zuo-Feng Xu, Hui-Xiong Xu et al.: Renal Cell Carcinoma and Renal Angiomyolipoma: Differential Diagnosis with Real-Time Contrast-Enhanced Ultrasonography. J Ultrasound Med 2010;29:709-717.

52. Gill IS, Aron M, Gervais DA, Jewett MAS. Small Renal Mass. New England Journal of Medicine 2010;362:624-634.

53. Bertin EJ: Mémoire pour servir al'histoire des reins. In: Histoire l'Académie Royale des Sciences. Paris: Académie Royale des Sciences. , 1744; 77-111.

54. Kara M, Tuma J.: [The forms and frequency of renal parenchymal cones]. Praxis 2014;103:199-202.

55. Hajdu SI, Foote FW: Angiomyolipoma of the kidney: report of 27 cases and review of the literature. J Urol. 1969;102:396-401.

56. Rule AD, Sasiwimonphan K, Lieske JC, Keddis MT, Torres VE, Vrtiska TJ: Characteristics of renal cystic and solid lesions based on contrast-enhanced computed tomography of potential kidney donors. Am J Kidney Dis. 2012;59.

57. Fujii Y AJ, Oka K, Tosaka A, Takehara Y Benign renal tumors detected among healthy adults by abdominal ultrasonography. Eur Urol. 1995;27.

58. Boeckmann W, JakseG: Nierenzellkarzinom. In: Rüben H, ed. Uroonkologie. Berlin, Heidelberg: Springer, 1997; 25-26.

59. Brenner DJ, Hall EJ. Computed Tomography : An Increasing Source of Radiation Exposure. New England Journal of Medicine 2007;357:2277-2284.

60. Bertolotto M, Cicero C, Catalano O, Currò F, Derchi LE. Solid Renal Tumors Isoenhancing to Kidneys on Contrast-Enhanced Sonography: Differentiation From Pseudomasses. Journal of Ultrasound in Medicine 2018;37:233-242.

61. Tuma J, Moch H, Stuckmann G, Gysel W, Serra AL. Two in One: Epithelioid angiomyolipoma within a classic kidney angiomyolipoma - a case report. BMC Nephrol 2018;19:123.

62. Silverman SG, Israel GM, Herts BR, Richie JP. Management of the Incidental Renal Mass. Radiology 2008;249:16-31.

63. Silverman SG, Gan YU, Mortele KJ, Tuncali K, Cibas ES. Renal Masses in the Adult Patient: The Role of Percutaneous Biopsy. Radiology 2006;240:6-22.

64. Aytac SK, Yigit H, Sancak T, Ozcan H. Correlation between the diameter of the main renal artery and the presence of an accessory renal artery: sonographic and angiographic evaluation. J Ultrasound Med 2003;22:433-439.

65. Staub D, Canevascini R, Huegli RW, Aschwanden M, Thalhammer C, Imfeld S, Singer E, et al. Best Duplex-Sonographic Criteria for the Assessment of Renal Artery Stenosis - Correlation with Intra- Arterial Pressure Gradient. Ultraschall in der Medizin 2007:45-51.

66. Jian-Chu Li LW, Yu-Xin Jiang, Qing Da. Evaluation of Renal Artery Stenosis With Velocity Parameters of Doppler Sonography. J Ultrasound Med 2006;25:735–742.

67. The ASTRAL STUDY, I. Revascularization versus Medical Therapy for Renal-Artery Stenosis. The New England Journal of Medicine 2009;361:1953-1962.

68. Catalano O, Nunziata A, Altei F, Siani A. Suspected ureteral colic: primary helical CT versus selective helical CT after unenhanced radiography and sonography. AJR Am J Roentgenol. 2002;178:379-387.

69. Tuma J, Schwarzenbach HR. Die Sonographie bei Nierenkolik. Schweiz.Rundsch.Med Prax. 2004;93:1767-1774.

70. Craig M WS, Sagalowsky A, et al. Prognostic factors, recurrence, and survival in transitional cell carcinoma of the upper urinary tract: a 30-year experience in 252 patients. Urology 1998;52:594-601.

71. Hollerweger A, Macheiner P, Gritzmann N: Akute linksseitige Unterbauchschmerzen: Sonographische Differenzialdiagnose. Ultraschall in Med 2003;24:7-16.

72. Park SJ, Yi BH, Lee HK, Kim YH, Kim GJ, Kim HC. Evaluation of Patients With Suspected Ureteral Calculi Using Sonography as an Initial Diagnostic Tool: How Can We Improve Diagnostic Accuracy? Journal of Ultrasound in Medicine 2008;27:1441-1450.

73. Patlas M, Farkas A, Fisher D, Zaghal I, Hadas-Halpern I. Ultrasound vs CT for the detection of ureteric stones in patients with renal colic. The British Journal of Radiology 2001;74:901-904.

74. Sheafor DH, Hertzberg BS, Freed KS, Carroll BA, Keogan MT, Paulson EK, DeLong DM, et al. Nonenhanced Helical CT and US in the Emergency Evaluation of Patients with Renal Colic: Prospective Comparison. Radiology 2000;217:792-797.

75. Darge K, Heidemeier A. Moderne Ultraschalltechniken und ihre Anwendungen am kindlichen Harntrakt. Radiologe 2005;45:1101-1111.

76. Jequier S, Paltiel H, Lafortune M. Ureterovesical jets in infants and children: duplex and color Doppler US studies. Radiology 1990;175:349-353.

77. Dubbins PA, Kurtz AB, Darby J, Goldberg BB. Ureteric jet effect: the echographic appearance of urine entering the bladder. A means of identifying the bladder trigone and assessing ureteral function. Radiology 1981;140:513-515.

78. Smith-Bindman R, Aubin C, Bailitz J, Bengiamin RN, Camargo CA, Corbo J, Dean AJ, et al. Ultrasonography versus Computed Tomography for Suspected Nephrolithiasis. New England Journal of Medicine 2014;371:1100-1110.